

# CHALMERS



## Thermoacoustic heat pump as a possibility to increase the efficiency of a tumble dryer

HENRIK JOHANSSON

Department of Civil and Environmental Engineering  
*Division of Applied Acoustics*  
*Vibroacoustics Group*  
CHALMERS UNIVERSITY OF TECHNOLOGY  
Göteborg, Sweden 2007  
Master Thesis 2007:34

CHALMERS UNIVERSITY OF TECHNOLOGY  
SE 412 96 Göteborg, Sweden  
Phone: + 46 - (0)31 772 10 00  
Web: [www.chalmers.se](http://www.chalmers.se)

MASTER'S THESIS 2007:34

# Thermoacoustic heat pump as a possibility to increase the efficiency of a tumble dryer

Henrik Johansson

Department of Civil and Environmental Engineering  
*Division of Applied Acoustics*  
*Vibroacoustics Group*  
CHALMERS UNIVERSITY OF TECHNOLOGY  
Göteborg, Sweden 2007

Thermoacoustic heat pump as a possibility to increase the efficiency of a tumble dryer  
Henrik Johansson

© Henrik Johansson, 2007

Master's Thesis 2007:34

Department of Civil and Environmental Engineering  
Division of Applied Acoustics  
Vibroacoustics Group  
Chalmers University of Technology  
S-41296 Göteborg  
Sweden

Tel. +46(0)31-772 2200

Reproservice / Department of Civil and Environmental Engineering  
Göteborg, Sweden 2007

Thermoacoustic heat pump as a possibility to increase the efficiency of a tumble dryer  
Master's Thesis in the Master's programme in Sound and Vibration  
Henrik Johansson  
Department of Civil and Environmental Engineering  
Division of Applied Acoustics  
Vibroacoustics Group  
Chalmers University of Technology

## Abstract

The purpose of a thermoacoustic heat pump in a tumble dryer application is to increase the energy efficiency of the dryer. An increment of the energy efficiency of the dryer means an improvement of the energy mark, during drying of a standardized test load. To improve the energy mark from C to B the thermoacoustic heat pump has to give a net power contribution of 250W.

A prototype was designed to verify the calculated performance of the thermoacoustic heat pump. The results suffers from low electroacoustic efficiency in the driver and also low efficiency of the heat transfer in the heat exchangers. Without further development of the driver and heat exchanger it is hard to determine the possible performance of the thermoacoustic heat pump.

**Keywords:** Thermoacoustic, Heat Pump, Tumble Dryer, Efficiency, Resonance, Stack, Heat Exchanger, Drive Ratio



# Contents

<b>Abstract</b>	<b>iii</b>
<b>Contents</b>	<b>vi</b>
<b>Notations</b>	<b>vii</b>
<b>1 Introduction</b>	<b>1</b>
1.1 Project description . . . . .	2
1.1.1 Goal . . . . .	2
1.1.2 Purpose . . . . .	2
1.1.3 Limitations . . . . .	2
<b>2 Tumble Dryer and the thermoacoustic heat pump</b>	<b>3</b>
2.1 Tumble dryer (Condenser) . . . . .	3
2.2 Energy labeling . . . . .	4
2.3 Thermoacoustic heat pump . . . . .	4
2.4 Possible application with a tumble dryer . . . . .	7
<b>3 Thermoacoustics</b>	<b>9</b>
3.1 Performance . . . . .	9
3.1.1 Coefficient of performance . . . . .	9
3.2 Rott's equation . . . . .	10
3.2.1 Energy flow . . . . .	12
3.3 Working gas . . . . .	12
3.3.1 Penetration depth . . . . .	13
3.3.2 Prandtl number . . . . .	13
3.4 Hardware . . . . .	13
<b>4 Design of the thermoacoustic heat pump</b>	<b>17</b>
4.1 Method and approximations . . . . .	17
4.1.1 DeltaE software . . . . .	20
4.2 Design choices . . . . .	21
4.2.1 Working gas . . . . .	21

4.2.2	Stack . . . . .	21
4.2.3	Driver . . . . .	22
4.2.4	Resonator . . . . .	22
4.2.5	Heat exchangers . . . . .	23
4.3	Final choices . . . . .	24
4.3.1	Calculations . . . . .	25
4.3.2	Measurement set-up . . . . .	27
<b>5</b>	<b>Measurements</b>	<b>31</b>
5.1	Calibration . . . . .	31
5.1.1	Pressure transducer . . . . .	31
5.1.2	Thermometers . . . . .	31
5.1.3	Water pumps . . . . .	32
5.2	Procedure . . . . .	33
5.3	Results . . . . .	34
5.3.1	Resonance . . . . .	34
5.3.2	Temperature difference depending on input power . . . . .	36
5.3.3	Helium . . . . .	36
5.3.4	Drive ratio . . . . .	36
5.3.5	Efficiency of heat exchangers . . . . .	39
<b>6</b>	<b>Discussion and conclusion</b>	<b>41</b>
6.1	Future work . . . . .	41
	<b>References</b>	<b>43</b>
<b>A</b>	<b>Appendix</b>	<b>45</b>
A.1	DeltaE Programs . . . . .	45
A.2	Measurements . . . . .	54

# Notations

## English letters

$A$	Area
$a$	Speed of sound
$B$	Block ratio or porosity
$C$	Energy consumption
$c_p$	Specific heat capacity
$D$	Drive ratio
$d$	Diameter
$f$	Frequency, Rott's function
$H$	Total power
$i$	$\sqrt{-1}$
$K$	Thermal conductivity
$k$	Wave number
$L$	Length
$l$	Half the thickness of the plates in the stack
$p$	Pressure
$Q$	Heat quantity
$R$	Impedance
$r$	Radius
$T$	Temperature
$t$	Time
$U$	Volume flow rate
$u$	Velocity
$V$	Voltage
$W$	Work, Acoustic power, Input power
$x$	Position
$y_0$	Half the spacing between the plates in the stack

## Greek letters

$\Gamma$	Operation parameter
$\gamma$	Ratio of isobaric to isochoric specific heats
$\Delta$	Big difference
$\delta$	Penetration depth



$\Lambda$	$= 1 - \delta_v / r_h + \delta_v^2 / 2r_h^2$
$\lambda$	Wavelength
$\mu$	Dynamic viscosity
$\pi$	3.14159...
$\rho$	Density
$\sigma$	Prandtl number
$\omega$	angular frequency

### Subscripts

$h$	Hydraulic
$m$	Mean
$C$	Cold
$H$	Hot
$L$	Loudspeaker
$s$	Stack
$w$	Water
$\kappa$	Thermal
$v$	Viscous
$crit$	Critical
$in$	Input
$out$	Output

# 1 Introduction

Today almost every tumble dryer has a C mark for the energy labeling during drying of a standardized test load. A tumble dryer (condenser) uses a condensing package where hot wet air goes through channels in one direction and cold dry air goes through other channels vertical from the other. A few dryers on the market have conventional heat pump systems for bringing out the humidity from the clothes. This is a very expensive method, so the idea is to use a thermoacoustic heat pump instead. Thermoacoustics is based on the interaction between pressure and temperature oscillations of a gas. Thermoacoustic refrigeration is a technology that uses high-amplitude sound waves in a pressurized gas to pump heat from one place to another. Advantages of thermoacoustic heat pumps is no sliding parts, it is environmentally safe and low cost. The big drawback is the efficiency.

Modern research and development of thermoacoustic systems is largely based upon the work of Rott and later Garrett and Swift. The most efficient thermoacoustic devices built to date have a relative Carnot efficiency approaching 40%, which is comparable with domestic vapor compression systems and in most cases superior to automotive internal combustion engines [9].

An animated introduction to thermoacoustic refrigeration can be seen at the homepage of the ice-cream manufacturer Ben & Jerry [11].

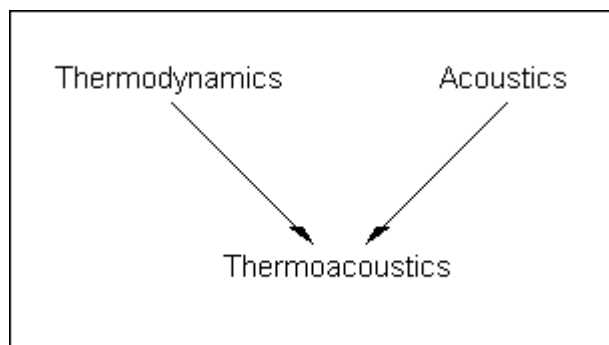


Figure 1.1: Thermoacoustics is the interaction of thermodynamics and acoustics.

## **1.1 Project description**

### **1.1.1 Goal**

The goal of this thesis is to investigate the possibility to use a thermoacoustic heat pump to increase the efficiency of a tumble dryer. The thesis is in cooperation with ASKO CYLINDA AB .

### **1.1.2 Purpose**

The thesis will aim for the thermoacoustic heat pump to reach a desired efficiency. The purpose of the thermoacoustic heat pump in application with a tumble dryer, is to increase the energy efficiency of a tumble dryer to improve the energy mark.

### **1.1.3 Limitations**

The thesis includes design and development of a thermoacoustic heat pump prototype to verify calculations with measurements. The primary aim is the performance of the thermoacoustic heat pump. Other practical issues like dimensions to fit the heat pump in the tumble dryer is not taken into consideration.

## 2 Tumble Dryer and the thermoacoustic heat pump

The purpose of the thermoacoustic heat pump is to increase the efficiency of a tumble dryer. This chapter will give an insight to the basic principle of a tumble dryer and the energy labeling system. The chapter will also explain the basic principle and parts of a thermoacoustic heat pump.

### 2.1 Tumble dryer (Condenser)

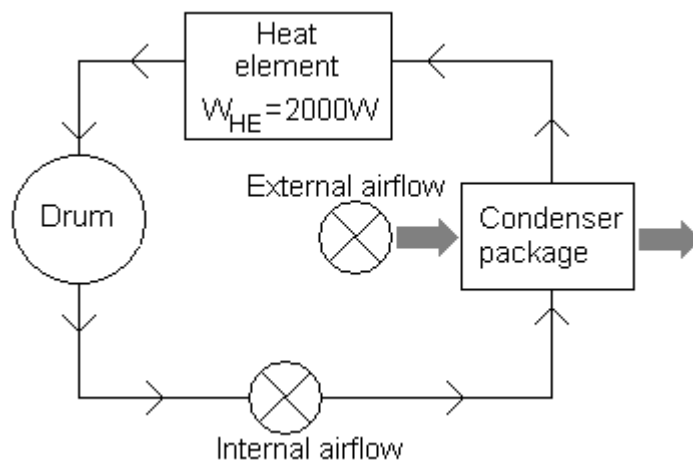


Figure 2.1: Block diagram of the closed system in the tumble dryer. An internal airflow transports the water vapor from the drum to the condenser package, which is cooled with an external room airflow.

A tumble dryer (condenser) can be modeled in blocks as a closed system as shown in figure 2.1. The hot air absorbs moisture from the wet clothes and an internal airflow transports the water vapor from the drum to the condenser package. In the condenser package the internal airflow is cooled with an external room airflow at room temperature to release the water.

## 2.2 Energy labeling

Tumble dryers are labeled with an energy mark according to their energy consumption. The labeling is based on directives from the European Union (EU) and is obligatory for all members in the EU. The labeling is based on measurements from the manufacturer during drying of a standardized test load according to a European standard. In Sweden this is controlled by the Swedish Energy Agency [8]. Tumble dryers are labeled with different marks on a scale from A to G showed in table 2.1 according to their energy consumption, with A-rating meaning the lowest energy consumption.

Mark	Energy consumption C [kWh/kg]
A	$C \leq 0.55$
B	$0.55 < C \leq 0.64$
C	$0.64 < C \leq 0.73$
D	$0.73 < C \leq 0.82$
E	$0.82 < C \leq 0.91$
F	$0.91 < C \leq 1.00$
G	$C > 1.00$

Table 2.1: Labeling index of energy consumption for a condenser dryer during drying of a standardized test load.

The aim of the investigation in this thesis is to see if it is possible to advance from a C to B mark by introducing a thermoacoustic heat pump. The heat element in figure 2.1 is supplied with electric power  $W_{HE}$  which has to be reduced with a factor  $C_B/C_C$ .

$$W_{HE} \left(1 - \frac{C_B}{C_C}\right) = \Delta W_{HP} \quad (2.1)$$

$\Delta W_{HP}$  is the power to be supplied by the thermoacoustic heat pump. Inserting values from table 2.1 gives,

$$\Delta W_{HP} = 2000W \left(1 - \frac{0.64}{0.73}\right) \approx 250W$$

So, 250W is the aim of the performance in the design of the thermoacoustic heat pump.

## 2.3 Thermoacoustic heat pump

A heat pump requires work to move thermal energy from a cold source to a warmer heat sink [9]. A thermoacoustic heat pump uses acoustic work to move thermal energy. As gas particles oscillates back and forth they undergo a change in pressure and

temperature, this is given by the ideal law of gases,

$$pV = nRT \quad (2.2)$$

In free air the oscillations are purely adiabatic, meaning no heat is transferred to the surrounding media. But when gas particles oscillate close to a solid boundary, heat is exchanged locally between the gas and the surrounding media.

A simple thermoacoustic heat pump, figure 2.2, use a standing wave field and a resonator fitting a half wavelength, so the length of the resonator is related to the wavelength as

$$L_{resonator} = \frac{\lambda}{2} \quad (2.3)$$

The resonator has two closed hard ends, so that the particle velocity  $u_1$  is zero and the pressure  $p_1$  is maximal at the ends. A driver is attached to one of the ends to supply acoustic work  $W$  and maintain a standing wave in the resonator.

A series of solid plates, referred to as a stack, are placed inside the resonator somewhere between a pressure maximum and minimum. The plates are placed parallel to each other and spaced closely together leaving small channels between them. This allows local heat exchange between gas and the solid and the oscillations are no longer adiabatic. Heat is supplied to the solid at high pressure and removed at low pressure. When a gas parcel is compressed the temperature of the parcel increases and rises above the local temperature of the solid and heat is transferred from the gas parcel to the solid. Through this local heat exchange mechanism, heat will be pumped from one side of the stack to the other leaving one side cold and one side hot. To supply and extract the heat from the ends of the stack, a heat exchanger is placed on

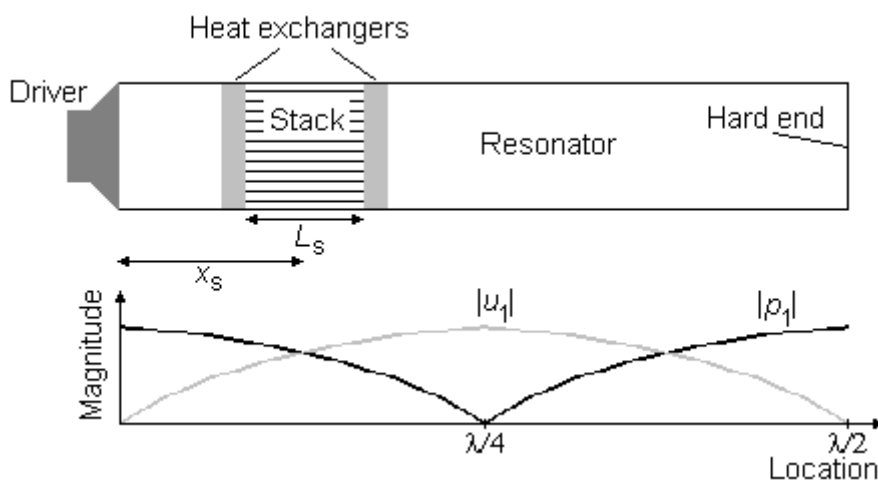


Figure 2.2: Schematic of a half wavelength standing wave thermoacoustic heat pump.

both sides of the stack. The heat exchangers are made with high thermally conductive material.

The part magnified in the stack in figure 2.3.a shows how the gas parcels supply heat to the solid at high pressure and remove heat at low pressure as the particles oscillate back and forth. A chain of oscillating gas parcels lead to a temperature gradient in the direction of the oscillating particles. A chain of gas parcels delivering the heat taken from the cold heat exchanger to the hot heat exchanger is illustrated in figure 2.3.b.

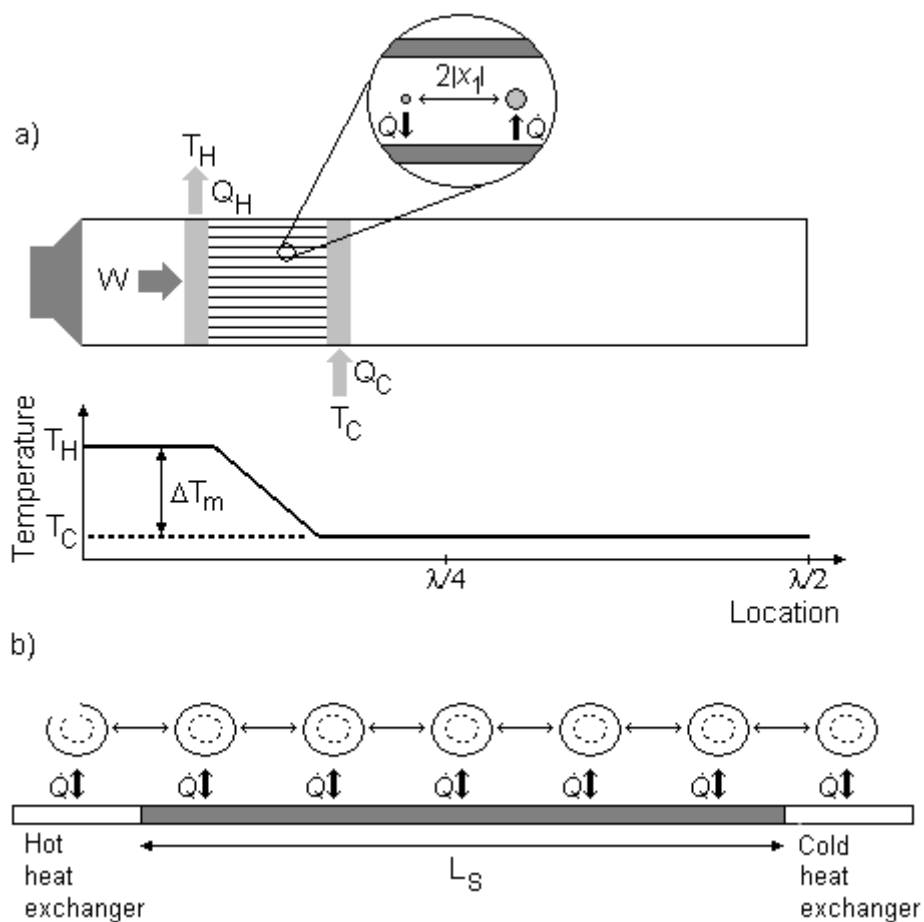


Figure 2.3: The heat pumping mechanism magnified. a) Heat is supplied to the solid at high pressure and removed at low pressure. b) A chain of gas parcels deliver the heat taken from the cold heat exchanger to the hot heat exchanger.

## 2.4 Possible application with a tumble dryer

Figure 2.4 shows a possible application of the thermoacoustic heat pump in a tumble dryer. The heat pump will "pump" thermal energy from the air entering the condenser package to the air exiting it. This is just a possibility for future application and will not be investigated and evaluated in this thesis.

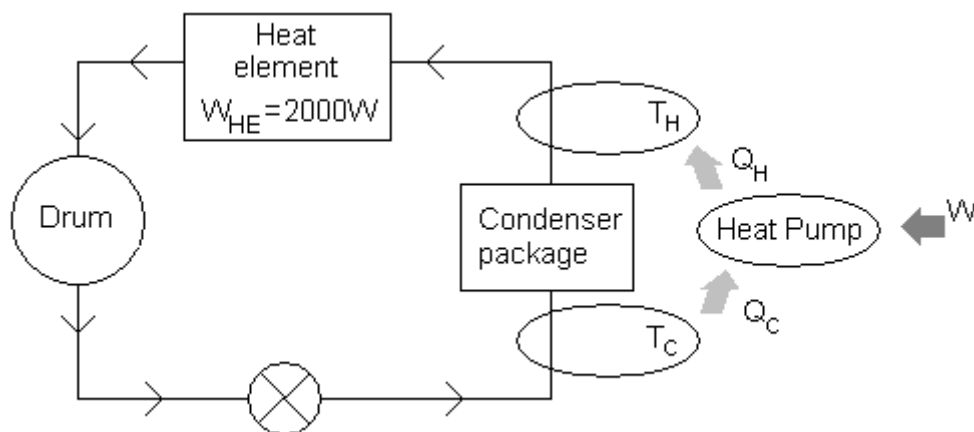


Figure 2.4: Possible application of the thermoacoustic heat pump in a tumble dryer.





# 3 Thermoacoustics

The basic principle of a heat pump is to remove a heat quantity  $Q_C$  at a low temperature  $T_C$  and supply a heat quantity  $Q_H$  at a high temperature  $T_H$  and work  $W$  is used to accomplish this process [4]. So a thermoacoustic heat pump use acoustic work  $W$  to pump heat from the cold side to the hot side of the stack.

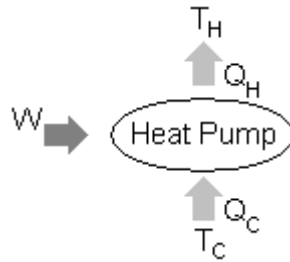


Figure 3.1: Basic principle of a thermoacoustic heat pump.

## 3.1 Performance

The first law of thermodynamics, simple energy conservation, states that for a heat pump at steady state conditions,

$$Q_H - Q_C - W = 0 \tag{3.1}$$

The second law of thermodynamics states for the same heat pump,

$$\frac{Q_C}{T_C} - \frac{Q_H}{T_H} \geq 0 \tag{3.2}$$

### 3.1.1 Coefficient of performance

The performance parameter for heat pumps is called coefficient of performance (*COP*). For heat pumps the *COP* is defined as the ratio of the desired heat  $Q_H$ , to the net work  $W$  needed. With help of the first law of thermodynamics, equation (3.1), the expression for the *COP* becomes,

$$COP = \frac{Q_H}{W} = \frac{Q_H}{Q_H - Q_C} \tag{3.3}$$

Combining the expression to the right in equation 3.3 and equation 3.2 gives

$$COP \leq \frac{T_H}{T_H - T_C} \quad (3.4)$$

The expression to the right in equation 3.4 is the Carnot *COP* which is the ideal and maximal performance for a heat pump. It is desirable that the *COP* have a value that is as high as possible. Looking at equation 3.4 we can see that the *COP* for a heat pump is always larger than unity and that small temperature difference will give higher *COP*.

## 3.2 Rott's equation

Equation (3.5) and (3.6) shows the momentum and continuity equation of ordinary lossless equations of acoustics

$$\frac{dp_1}{dx} = -j\omega\rho_m u_1 \quad (3.5)$$

$$\frac{du_1}{dx} = -j\omega \frac{1}{\gamma p_m} p_1 \quad (3.6)$$

where  $p_1$  is the oscillating pressure and  $u_1$  is the oscillating particle velocity. Below is the thermoacoustic versions of the momentum and continuity equation [2],

$$\frac{dp_1}{dx} = -\frac{j\omega\rho_m}{1-f_v} u_1 \quad (3.7)$$

$$\frac{du_1}{dx} = -\frac{j\omega}{\gamma p_m} [1 + (\gamma - 1)f_\kappa] p_1 + \frac{(f_\kappa - f_v)}{(1-f_v)(1-\sigma)} \frac{1}{T_m} \frac{dT_m}{dx} u_1 \quad (3.8)$$

Combining equation (3.7) and equation (3.8) gives Rott's wave equation,

$$[1 + (\gamma - 1)f_\kappa] p_1 + \frac{\gamma p_m}{\omega^2} \frac{d}{dx} \left( \frac{1-f_v}{\rho_m} \frac{dp_1}{dx} \right) - \frac{a^2}{\omega^2} \frac{f_\kappa - f_v}{1-\sigma} \frac{1}{T_m} \frac{dT_m}{dx} \frac{dp_1}{dx} = 0 \quad (3.9)$$

This is the wave equation for  $p_1$  in the presence of a mean temperature gradient  $dT_m/dx$  in the stack. This was first obtained by Rott, for an ideal gas and stack .

The  $f$ -function, figure (3.2), depends on the specific channel geometry and materials properties under consideration [2]. For geometry with parallel plates with spacing  $2y_0$ ,

$$f = \frac{\tanh((1+j)y_0/\delta)}{(1+i)y_0/\delta} \quad (3.10)$$

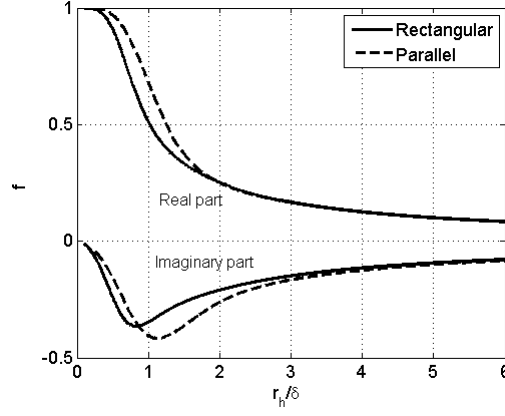


Figure 3.2: The  $f$ -function for parallel and rectangular stack geometry ( $2y_0=2z_0$ ). Using  $\delta_v$  gives  $f_v$  and using  $\delta_\kappa$  gives  $f_\kappa$ .

For geometry with rectangular channels of dimensions  $2y_0 \times 2z_0$ ,

$$f = 1 - \frac{64}{\pi^4} \sum_{m,n \text{ odd}} \frac{1}{m^2 n^2 C_{mn}} \quad (3.11)$$

where

$$C_{mn} = 1 - j \frac{\pi^2 \delta^2}{8y_0^2 z_0^2} (m^2 z_0^2 + n^2 y_0^2) \quad (3.12)$$

Using  $\delta_v$  gives  $f_v$  and using  $\delta_\kappa$  gives  $f_\kappa$ , in equation 3.10 and 3.11.

The work  $W$  required to pump heat referrers to the acoustic power used or absorbed in the stack. Swift [2] has derived an expression for the total power in the stack,

$$\begin{aligned} H = & \frac{A_g}{2} \text{Re} \left[ p_1 \langle \tilde{u}_1 \rangle \left( 1 - \frac{f_\kappa - \tilde{f}_v}{(1 + \sigma)(1 - \tilde{f}_v)} \right) \right] \\ & + \frac{A_g \rho_m c_p |\langle u_1 \rangle|^2}{2\omega(1 + \sigma^2) |1 - f_v|^2} \text{Im}[f_\kappa + \sigma \tilde{f}_v] \frac{dT_m}{dx} \\ & - (A_g K + A_s K_s) \frac{dT_m}{dx} \end{aligned} \quad (3.13)$$

and the acoustic work absorbed in the stack per unit length,

$$\begin{aligned} \frac{dW}{dx} = & -\frac{A_g}{2} \left( \frac{\omega \rho_m \text{Im}[-f_v]}{|1 - f_v|^2} |\langle u_1 \rangle|^2 + \frac{\omega(\gamma - 1) \text{Im}[-f_\kappa]}{\gamma p_m} |p_1|^2 \right) \\ & + \frac{A_g}{2} \frac{1}{(1 - \sigma) T_m} \frac{dT_m}{dx} \text{Re} \left[ \frac{(f_\kappa - f_v)}{(1 - f_v)} \tilde{p}_1 \langle u_1 \rangle \right] \end{aligned} \quad (3.14)$$

### 3.2.1 Energy flow

Figure (3.3) shows the energy flow in the heat pump, neglecting resonator losses. Applying a control volume and using energy conservation of the first law we can look at how the energy flows in the stack. The acoustic power  $W$  is constant from the driver to the left side of the stack, decreases to zero in the stack as acoustic power is absorbed to pump heat from the right to the left side of the stack and is constant at zero from the right side of the stack to the end of the resonator. The total power  $H$  is constant in the resonator regions and in the stack. It rises and falls discontinuously as heat is supplied and extracted at the heat exchangers. The heat  $Q_C$  supplied to the cold heat exchanger is equal to the total power in the stack and the heat  $Q_H$  extracted from the hot heat exchangers is the sum of the total power and the acoustic power absorbed in the stack.

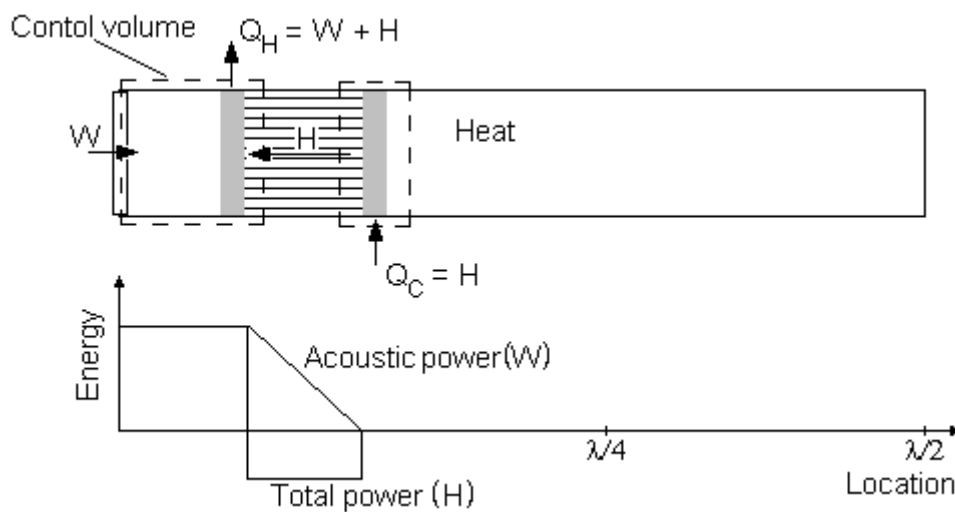


Figure 3.3: The total power  $H$  is constant in the resonator regions and in the stack. The discontinuities in the total power  $H$  are the heat transferred at the heat exchangers. The acoustic power  $W$  is constant in the resonator regions and decreases to zero in the stack. The heat  $Q_H$  extracted from the hot heat exchanger is the sum of the total power and the acoustic power.

### 3.3 Working gas

The choice of gas involves issues like power, efficiency and convenience. Parameters like thermal and viscous penetration depth and Prandtl number are important. Power is related to the gas as  $H \propto \rho_m a A$ , thus a gas with high sound speed is desired

[3]. High thermal conductivity is desired to lower the heat conduction through the stack. It is also desired to minimize the viscous effects. Light gases and high mean static pressure put demands on the construction.

### 3.3.1 Penetration depth

The thermal and viscous penetration depth are lengths perpendicular to the oscillations of the gas. At a distance much greater than the thermal penetration depth from the solid boundary, the gas feels no thermal contact with the solid boundaries. Close to a solid boundary the displacement of gas particles is too small and the viscous effect are strong. The thermal penetration depth  $\delta_\kappa$  and viscous penetration depth  $\delta_\nu$  are defined as,

$$\delta_\kappa = \sqrt{\frac{K}{\pi f \rho_m c_p}} \quad (3.15)$$

$$\delta_\nu = \sqrt{\frac{\mu}{\pi f \rho_m}} \quad (3.16)$$

where  $K$  is the thermal conductivity,  $\mu$  is the dynamic viscosity,  $c_p$  is the specific heat,  $\rho_m$  is the mean density and  $f$  is the operating frequency. The density  $\rho_m$  is proportional to the mean static pressure  $p_m$ , so high mean static pressure reduces  $\delta_\kappa$  and  $\delta_\nu$ . Increasing the static pressure leads to smaller plate spacing in the stack for optimal thermal contact between gas and solid.

### 3.3.2 Prandtl number

Prandtl number is a dimensionless parameter describing the ratio between viscous and thermal effects and is defined as,

$$\sigma = \left(\frac{\delta_\nu}{\delta_\kappa}\right)^2 = \frac{\mu c_p}{K} \quad (3.17)$$

It is desired to keep the ratio as low as possible to minimize the viscous effects.

## 3.4 Hardware

The choice of hardware in the heat pump involves issues like fabrication, efficiency and choice of material properties. Stacks should provide local heat capacity for the gas, while heat exchangers should allow high heat conduction. Small spacings in the stack and heat exchangers means challenging fabrication.

## Stack

The heart of the heat pump is the stack and this where the actual heat pumping process occurs. The stack provides local heat capacity for the working gas and should also minimize heat conduction in the direction of the oscillating particles. The stack should have a high heat capacity and low thermal conductivity and it should also minimize dissipation of acoustic work. The position of the stack determines the proportion of viscous losses to the losses due to thermal relaxation effects between the gas and the stack. It is usually placed a distance of  $\lambda/20$ - $\lambda/8$  from a pressure maximum. The amount of acoustic work absorbed in the stack is dependent on the length of the stack.

The stack should not interfere with the wave field in the resonator. The porosity of the stack, also called the block ratio, is defined as

$$B = \frac{A_{gas}}{A_{tot}} \quad (3.18)$$

where  $A_{gas}$  is the cross-sectional area of the gas in the stack,  $A_{tot}$  is the total cross-sectional area of the resonator. The block ratio for a stack with parallel plates is given by,

$$B_{parallel} = \frac{y_0}{y_0 + l} \quad (3.19)$$

where  $y_0$  is half the plate spacing and  $l$  is half the plate thickness, see figure (3.4). Larger plate spacing allows easier stack and heat exchanger fabrication. Half the plate spacing  $y_0$  should be larger than the viscous penetration depth  $\delta_v$  and close to or just above thermal penetration depth  $\delta_\kappa$ , to get minimal viscous dissipation but still good thermal contact.

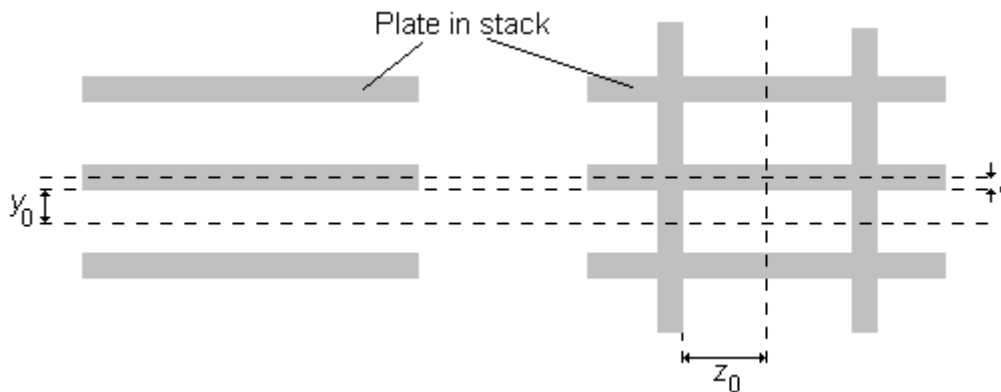


Figure 3.4: Shown on the left is a stack with parallel plates spaced with  $2y_0$  and plate a thickness of  $2l$ . Shown on the right is a stack with rectangular channel geometry and with dimensions  $2y_0 \times 2z_0$ .

For a stack with rectangular channels the block ratio is

$$B_{\text{rectangular}} = \frac{y_0 z_0}{(y_0 + l)(z_0 + l)} \quad (3.20)$$

with square channels  $z_0=y_0$ , the block ratio becomes

$$B_{\text{square}} = \frac{y_0^2}{(y_0 + l)^2} \quad (3.21)$$

## Resonator

A standing wave heat pump is convenient to use because of its simple construction. The resonator can either be a tube fitting a half wavelength standing wave (equation 2.3) or a tube fitting a quarter wavelength with a buffer volume. The length of the resonator is dependent on the working gas and operating frequency. High sound speed lead to a longer resonator.

## Driver

The driver has to produce the amount of acoustic power absorbed in the stack. The operating frequency used is usually chosen to be between 200-500Hz as a compromise between plate spacing in the stack and length of the resonator.

The electroacoustic efficiency of a commercial hifi speaker is very low, but it is still convenient to use because of its low cost and availability. The driver has to handle high power, have a large magnet (high Bl-factor) and a stiff membrane. The speaker can be modified by adding a stiffer membrane to handle high pressure amplitudes. It is shown by Tijani [4] that when the mechanical resonance of the driver is matched to the resonance of the resonator an electroacoustic efficiency of 33% can be reached in a wide frequency range. Thermoacoustic theory is based on acoustic approximations and small amplitudes, but when the heat pump is operating at high amplitudes nonlinearities such as turbulence, streaming and harmonic shocks can arise.

## Heat exchangers

Heat exchangers extract the heat from the hot side of the stack and supply heat at the cold side of the stack. The design challenge is to make good thermal contact between two flowing systems while causing minimal pressure drop in either stream. The gas parcels at the ends of the stack are at the end of the chain of gas parcels involved in the heat pumping mechanism. The gas parcels oscillate back and forth between the stack and the heat exchanger, so the optimal length of the heat exchangers corresponds



to twice the particle displacement amplitude, see figure 3.5. The displacement  $x_1$  is given by,

$$x_1 = \frac{u_1}{\omega} = \frac{\hat{p}_1}{\omega \rho_m a} \sin(kx) \quad (3.22)$$

where  $\hat{p}_1$  is the peak amplitude of the oscillating pressure  $p_1$  and  $x$  the position of the heat exchanger.

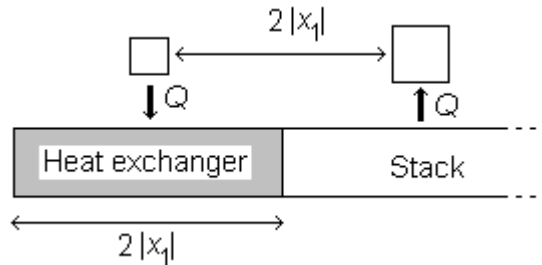


Figure 3.5: An illustration of the optimal length of the heat exchanger corresponding to twice the peak displacement amplitude of the oscillating particles.

## 4 Design of the thermoacoustic heat pump

The design of the heat pump involves many difficult and practical issues. One of the aims with this design is to gain useful experience in the design process. The design of stacks and heat exchangers is made difficult by small plate spacings. The use of different gases and high mean static pressure puts demands on safety and the construction of the resonator. Approximations can be hard to match in reality, due to low efficiency of electroacoustic drivers and heat exchangers and other losses in the system, such as losses through the resonator and junctions.

### 4.1 Method and approximations

The boundary layer approximation assumes wide open channels in the stack ( $y_0 \gg \delta_\kappa$ ,  $y_0 \gg \delta_v$  and  $l \gg \delta_s$ ). The short stack approximation assumes the stack length is small compared to the wavelength ( $\lambda \gg L_s$ ), so that the pressure and velocity does not change considerably along  $x$ -direction of the stack. Then all  $x$ -dependent and  $T_m$ -dependent variables can be regarded as constant. Swift [2] and Tijani [4] makes similar approximation. The standing wave acoustic pressure is given by

$$p_1 = \hat{p}_1 \cos(kx) \quad (4.1)$$

and the mean velocity

$$\langle u_1 \rangle = j \frac{1}{B} \frac{\hat{p}_1}{\rho_m a} \sin(kx) \quad (4.2)$$

The factor  $1/B$  is used, due to the continuity of volumetric velocity at the boundary of the stack. This requires that the velocity is higher in the stack. For the boundary layer approximation the  $f$ -function becomes,

$$f = \frac{(1-j)\delta}{2r_h} \quad (4.3)$$

With these assumptions the expression in equation 3.13 reduces to,

$$H = \frac{A_g \delta_\kappa |p_1| |\langle u_1 \rangle|}{4r_h (1+\sigma) \Lambda} \left( \Gamma \frac{1 + \sqrt{\sigma} + \sigma}{1 + \sqrt{\sigma}} - 1 - \sqrt{\sigma} + \frac{\delta_v}{r_h} \right) - (A_g K + A_s K_s) \frac{dT_m}{dx} \quad (4.4)$$

and equation (3.14) reduces to,

$$\Delta W = \frac{A_g L_s}{4r_h} \left[ \frac{(\gamma - 1)|p_1|^2 \delta_\kappa \omega}{\gamma p_m} \left( \frac{\Gamma}{(1 + \sqrt{\sigma})\Lambda} - 1 \right) - \frac{\rho_m |\langle u_1 \rangle|^2 \delta_v \omega}{\Lambda} \right] \quad (4.5)$$

where

$$\Gamma = \frac{dT_m/dx}{\nabla T_{crit}} \quad (4.6)$$

$$\nabla T_{crit} = \frac{\omega A_g |p_1|}{\rho_m c_p |\langle u_1 \rangle|} \quad (4.7)$$

$$\Lambda = 1 - \frac{\delta_v}{r_h} + \frac{\delta_v^2}{2r_h^2} \quad (4.8)$$

$\Gamma$  defined in equation 4.6 is called the operation parameter. When  $dT_m/dx = \nabla T_{crit}$  ( $\Gamma=1$ ), heat is neither produced nor absorbed in the stack and  $\nabla T_{crit}$  is called the critical frequency which marks the breakpoint between heat pump and engine operation. Standing wave heat pumps have  $|dT_m/dx| < \nabla T_{crit}$  ( $\Gamma < 1$ ), where acoustics work is absorbed in the stack and standing wave engines have  $|dT_m/dx| > \nabla T_{crit}$  ( $\Gamma > 1$ ), where acoustic work is produced in the stack. The last term in equation 4.4 is due to heat conduction in the stack in the presence of a mean temperature gradient in the stack.

Ahlborn and Camire [7] has shown that a thermoacoustic heat pump delivers maximum heat power when it operates at 1/3 of the Carnot  $COP$  and the stack is about  $\lambda/8$  from a pressure maximum. This means that the aim of the operation parameter  $\Gamma$  should be close to 1/3. When a stack length is chosen  $\Gamma$  can be controlled by varying the temperature difference  $\Delta T_m$  between the hot and cold side of the stack.

Tijani derives a dimensionless expression using parameter normalization [4], which is also based on the boundary layer and short stack approximation. The dimensionless expression is useful to examine the dependence on the stack length and stack position. For example the stack length  $L_s$  and stack position  $x_s$  is normalized by the wave number  $k$ .

$$L_{sn} = kL_s \quad (4.9)$$

$$x_n = kx_s \quad (4.10)$$

Compared to Swifts approximation (equation 4.4 and 4.5) he assumes the thermal conductivity of the stack to be lower than the gas ( $K > K_s$ ) to neglect heat conduction

in the stack.

$$H_n = -\frac{\delta_{\kappa n} D^2 \sin(2x_n)}{8\gamma(1+\sigma)\Lambda} \left( \Gamma \frac{1+\sqrt{\sigma}+\sigma}{1+\sqrt{\sigma}} \right) - (1+\sqrt{\sigma}-\sqrt{\sigma}\delta_{\kappa n}) \quad (4.11)$$

$$\begin{aligned} \Delta W_n &= \frac{\delta_{\kappa n} L_{sn} D^2}{4\gamma} (\gamma-1) B \cos(x_n)^2 \left( \frac{\Gamma}{(1+\sqrt{\sigma})\Lambda} - 1 \right) \\ &- \frac{\delta_{\kappa n} L_{sn} D^2}{4\gamma} \frac{\sqrt{\sigma} \sin(x_n)^2}{B\Lambda} \end{aligned} \quad (4.12)$$

where

$$\Gamma = \frac{\Delta T_{mn} \tan(x_n)}{BL_{sn}(\gamma-1)} \quad (4.13)$$

$$\Lambda = 1 - \sqrt{\sigma}\delta_{\kappa n} + \frac{1}{2}\sigma\delta_{\kappa n}^2 \quad (4.14)$$

$$D = \frac{p_1}{p_m} \quad (4.15)$$

D is called the drive ratio, where the  $p_1$  is the standing wave peak amplitude of the oscillating pressure and  $p_m$  is the mean static pressure. The total power  $H$  and the acoustic work  $\Delta W$  is normalized by  $1/\rho_m a A$ ,

$$H_n = H/\rho_m a A \quad (4.16)$$

$$\Delta W_n = \Delta W/\rho_m a A \quad (4.17)$$

The *COP* is calculated by,

$$COP = \frac{H_n + \Delta W_n}{\Delta W_n} = \frac{H_n}{\Delta W_n} + 1 \quad (4.18)$$

The graphs displayed in figure 4.1 are calculated using the Tijani dimensionless normalization and helium as working gas. The temperature difference is chosen so the operation parameter  $\Gamma$  in the top right graph is below 1 ( $\Gamma < 1$ ) for all four stack positions. The aim of the operation parameter is about  $\Gamma=1/3$  as mentioned in the previous section. In the top left graph the *COP* is higher for a stack position close to a pressure maximum and there seems to be a maximum at each stack position. The bottom left graph shows how the total power in the stack increases and eventually flattens out with increasing stack length. In the bottom right graph it is clear that a longer stack absorbs more acoustic power. This explains why the *COP* decreases for longer stack lengths. It should be noted that the graphs in figure 4.1 is calculated with a parallel stack.

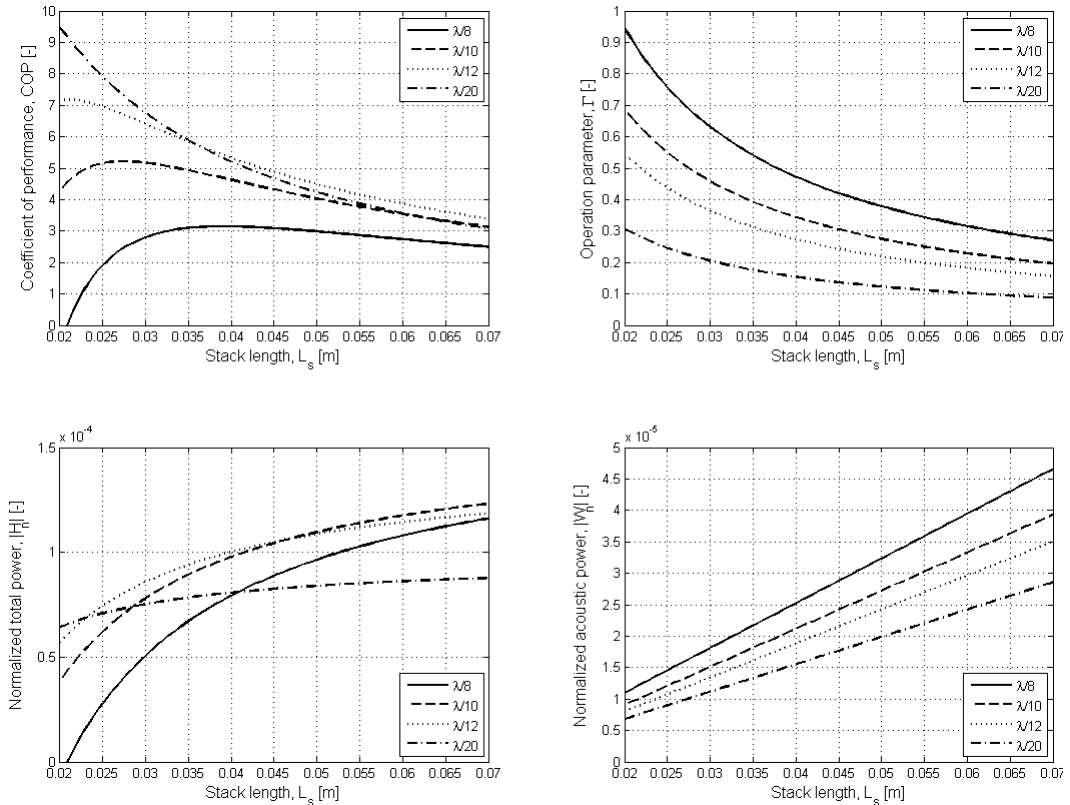


Figure 4.1: The graphs in these plots are calculated with the Tijani approximation (equation 4.12 and 4.13), at different stack positions. Gas properties of helium and a constant temperature difference of  $\Delta T_m = 8\text{K}$  between the hot and cold side of the stack is used.

#### 4.1.1 DeltaE software

A useful tool in the design process is the DeltaE software [5] (Design Environment for Low-amplitude ThermoAcoustic Engines). DeltaE is a partial differential equation solver which solves the one-dimensional wave equation based on the usual low-amplitude acoustic approximation and takes the thermal loss and viscous loss into consideration. It solves the wave equation in a gas or liquid, in a geometry given by the user, specified as a sequence of segments, such as ducts, compliances, transducers and thermoacoustic stacks. DeltaE does not include any nonlinear effects that arise at high amplitudes.

## 4.2 Design choices

I have chosen to design a half wavelength standing wave heat pump, which makes the design and construction process less challenging. The design choices are based on the boundary layer and short stack approximations.

### 4.2.1 Working gas

Helium was chosen as working gas because it has high sound speed, high thermal conductivity and low Prandtl number compared to air. Sound speed is proportional to power, high thermal conductivity is desired to lower heat conduction through the stack and low Prandtl number ( $\sigma$ ) decreases the influence of viscous effects. Although the heat pump is design for helium gas it will also be used with air. Table 4.1 shows a comparison between the gas properties of air and helium at a temperature of  $T=300\text{K}$ .

	Air	Helium	
a	347	1019	[m/s]
$c_p$	1005	5197	[J/kgK]
$K$	$26 \cdot 10^{-3}$	$152 \cdot 10^{-3}$	[W/Km]
$\mu$	$1.85 \cdot 10^{-5}$	$1.99 \cdot 10^{-5}$	[kg/sm]
$\sigma$	0.71	0.68	[-]

Table 4.1: Properties of air and helium calculated with a temperature of  $T_m=300\text{K}$ . The definition of Prandtl number is found in equation 3.17.

### 4.2.2 Stack

The stack used in the measurement set-up is a prefabricated stack made of Celcor<sup>TM</sup> [6] ceramic material and was available at the department. A prefabricated stack is convenient because it is one of the challenging factors in the fabrication process. Two stack pieces were available, one with a length of 2.5cm and the other a length of 4cm. This makes it possible to have three different lengths, 2.5cm, 4cm and 6.5cm. The stack length was chosen to 4cm and the stack position to  $\lambda/10$ . The choice is a compromise between power and efficiency. The stack has a diameter of 147mm and square channel geometry. The material properties and channel dimensions are shown in table 4.2 and a close-up of the channel geometry of the stack is shown in figure 4.2.

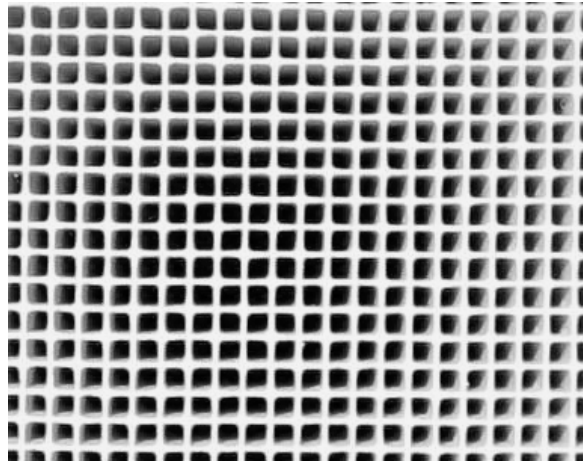


Figure 4.2: Close-up of the channel geometry in the stack.

$c_s$	616.2J/kgK
$K_s$	2.6W/Km
$y_0$	0.55mm
$l$	0.09mm
$B$	0.74

Table 4.2: Properties of the Celcor<sup>TM</sup> material and the dimensions of the channels in the stack.

### 4.2.3 Driver

The operating frequency of the driver was chosen to  $f=400\text{Hz}$  with helium as working gas. The driver Beyma 6B10 is a 6-inch PA loudspeaker and it was chosen to have a large magnet, low resonance frequency and high sensitivity. The diameter of the loudspeaker was chosen to fit the resonator and is mounted on the resonator as showed in figure 4.3. The manufacturer could not provide a datasheet for the driver, so matching of the mechanical resonance of the driver and the acoustic resonance of the resonator turned out to be too extensive and was not evaluated due to limitation in time.

### 4.2.4 Resonator

The resonator is designed to fit half the wavelength of the operating frequency. This gives the resonator a length of 1.274m with a frequency of  $f=400\text{Hz}$  and helium as working gas. The diameter of the resonator was chosen to fit the maximum diameter of the stack (147mm). The heat pump will be used with a static pressure of up to



Figure 4.3: The driver is mounted to the resonator and the box is then mounted separately over the back of the loudspeaker. The cable passage through the loudspeaker box has to be gastight. A copper block passes through the wall of the box, wires connect the block on the inside to the loudspeaker and on the outside to the amplifier.

4bar. For pressure equalization in front and back of the driver membrane the back of the loudspeaker is covered by a box. The volume of the box is dimensioned to have a resonance frequency below the operating frequency of the driver. Figure 4.4 shows how the equalization is solved in the design. A tube is mounted on the outside of the heat pump, from the resonator to the loudspeaker box. The valve where the resonator is pressurized and filled with gas is also located on the equalization tube. The tube also has an input for the manometer used to measure the static pressure in the resonator. The value of the static pressure is displayed on a Fluke multimeter with a sensitivity of 1mV/kPa. All the junctions also have to be gastight.

#### 4.2.5 Heat exchangers

The heat exchangers are made of 6mm copper tube wound into a spiral with about 18mm spacing as shown in figure 4.5. The spacing in the heat exchangers was chosen to have a block ratio close to the block ratio of the stack. It was calculated to  $B=0.75$  using equation 3.19. In the tube, water is circulating to supply and extract the heat



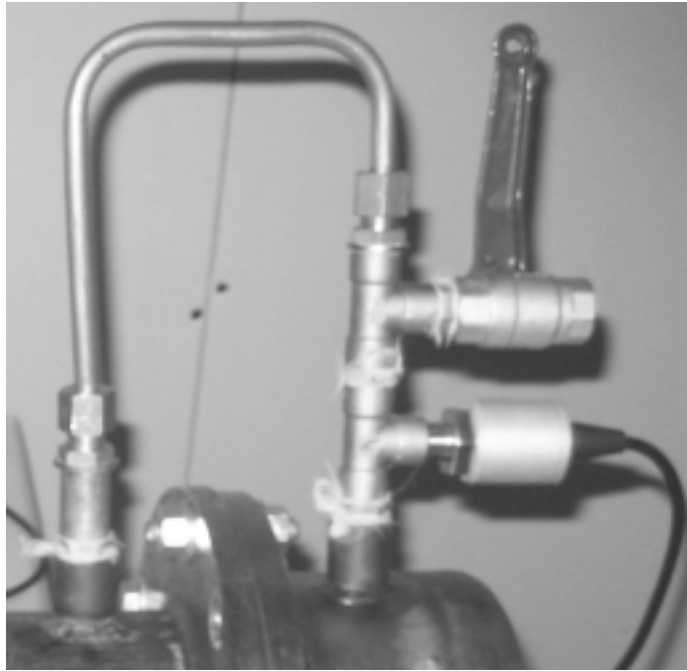


Figure 4.4: The pressure equalization tube, for pressure equalization in front and back of the loudspeaker. The valve on the top is where the resonator is pressurized and the valve on the bottom is where the manometer is connected to measure the static pressure.

at the heat exchangers. This requires two water pumps to circulate and control the velocity of the water, one for each heat exchanger.

### 4.3 Final choices

The design choices discussed in this chapter are summarized in table 4.3.

$f$	400Hz
$L_{resonator}$	1.274m
$L_s$	0.04m
$x_s$	0.25m
$d$	0.145m
Gas	Helium
$p_m$	1-4bar

Table 4.3: A summary of the design choices.

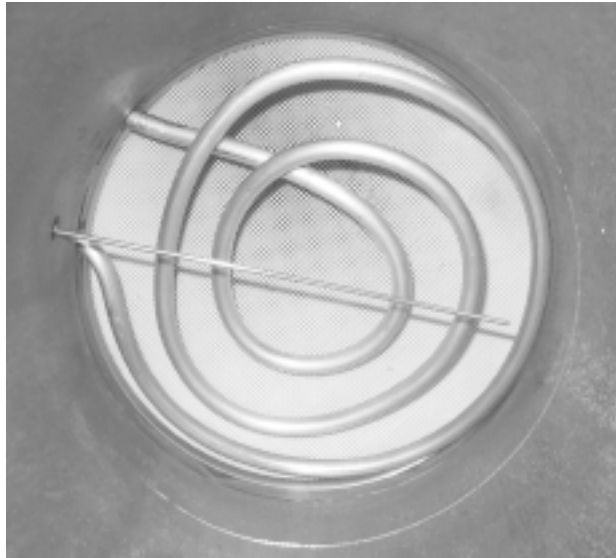


Figure 4.5: A picture looking into the resonator from the loudspeaker end. The picture shows the heat exchanger and the thermometer on the hot side of the stack.

### 4.3.1 Calculations

As discussed in chapter 2 the aim of the design is to reach a net power contribution of  $\approx 250\text{W}$ . The calculations in this section compare results based on the boundary layer and short stack approximation in section 4.1, with results obtained with calculations in DeltaE. The calculations use the final design choices summarized in table 4.3 and in the DeltaE model the heat exchangers have a length of 6mm and the same block ratio as the stack. The DeltaE models are included in appendix A.1.

#### Parallel stack

The results in table 4.4 is calculated with a parallel stack using the same plate spacing and plate thickness as given in table 4.2. This gives the stack a block ratio of  $B=0.86$ , which is a little higher than the stack used in the measurement set-up. The results show that the values obtained from the boundary layer approximation are overestimated compared to the results from the DeltaE model.

#### Rectangular stack

The results in table 4.5 are calculated with a rectangular stack and the same channel dimensions as used in the measurement set-up. Again the results show that the values obtained from the boundary layer approximation are overestimated.

		100kPa	200kPa	300kPa	400kPa
B.L./short stack	$H$	167W	252W	312W	361W
	$\Delta W$	37W	48W	57W	65W
	$Q_H$	204W	301W	369W	426W
	$COP$	5.6	6.2	6.5	6.6
DeltaE	$H$	104W	159W	202W	237W
	$\Delta W$	37W	46W	54W	62W
	$Q_H$	191W	269W	330W	382W
	$COP$	5.2	5.8	6.1	6.2

Table 4.4: Performance of the thermoacoustic heat pump calculated with the boundary layer (B.L.)/short stack approximation and DeltaE model. The final choices in table 4.3, gas properties of helium, parallel stack geometry, a drive ratio of  $D=0.05$  and a temperature difference of  $\Delta T_m=8\text{K}$  ( $\Gamma=0.34$ ) are used.

		100kPa	200kPa	300kPa	400kPa
B.L./short stack	$H$	93W	369W	540W	666W
	$\Delta W$	86W	120W	140W	156W
	$Q_H$	179W	489W	680W	822W
	$COP$	2.1	4.1	4.9	5.3
DeltaE	$H$	51W	120W	181W	236W
	$\Delta W$	77W	102W	106W	115W
	$Q_H$	153W	241W	323W	396W
	$COP$	1.9	2.4	3.0	3.4

Table 4.5: Performance of the thermoacoustic heat pump calculated with the boundary layer (B.L.)/short stack approximation and DeltaE model. The final choices in table 4.3, gas properties of helium, square stack geometry, a drive ratio of  $D=0.05$  and a temperature difference of  $\Delta T_m=7\text{K}$  ( $\Gamma=0.35$ ) are used.

The results obtained from the DeltaE model depend on the heat exchanger dimensions used. The results in table 4.6 instead use a heat exchanger length of 19mm, corresponding to twice the peak displacement amplitude. It shows that with longer heat exchangers more heat is extracted from the hot heat exchanger and more heat is also supplied to the cold heat exchanger.

	400kPa
$H$	339W
$\Delta W$	118W
$Q_H$	546W
$COP$	4.6

Table 4.6: The total power  $H$  and the acoustic power  $\Delta W$  calculated with DeltaE, the final choices in table 4.3 and a heat exchanger length of 19mm, corresponding to twice the peak displacement amplitude. The results can be compared with the values at 400kPa in table 4.5.

### Temperature

If we continue and look at the mean temperature inside the resonator. In table 4.7 we can see that the output heat is increased with increasing mean temperature. But the  $COP$  is fairly constant, which means that the increase in output heat is proportional to the absorbed acoustic power.

	300K	310K	320K	330K
$H$	339W	356W	372W	388W
$\Delta W$	118W	123W	128W	133W
$Q_H$	546W	571W	596W	620W
$COP$	4.6	4.6	4.7	4.7

Table 4.7: The total power  $H$  and the acoustic power  $\Delta W$  calculated with DeltaE, the final choices in table 4.3 and a heat exchanger length of 19mm, corresponding to twice the peak displacement amplitude. The mean temperature is varied to compare the output heat.

### 4.3.2 Measurement set-up

The prototype was built in the workshop at the Technical Research Institute of Sweden. During the construction of the prototype a few minor changes were made concerning the dimension of the resonator.

The resonator has a length of 1.38m which under ideal conditions gives an operating frequency of 370Hz using helium. The stack length is  $L_s=0.04\text{m}$  and the stack center position is at  $x_s=0.26\text{m}$ , which is close to  $\lambda/10\text{m}$ . The heat pump was tested to hold for a static pressure up to 6bar, but will only be used up to 4bar. The heat pump is built in four parts, one part is the loudspeaker box, one part is holding the stack showed in figure 4.8, one resonator part between the driver and the stack and one resonator part with a closed hard end. This makes it possible to replace and repair any defects on the equipment inside the resonator or defects on the resonator parts. It would also be possible to redesign the construction in several ways to increase the performance.

A pressure transducer is mounted in the resonator wall and is located close to the loudspeaker. The pressure transducer is a high sensitivity transducer that measures the oscillating pressure in the resonator. The transducer is used to determine the resonance frequency of the resonator and to determine the drive ratio at a certain input power.

Two thermometers are mounted through the resonator wall to measure the temperature of the air on both sides of the stack and a transmitter converts the signal from the thermometers to a voltage between 0-10V ( $1^\circ\text{C}=0.1\text{V}$ ,  $2^\circ\text{C}=0.2\text{V}$ , ...). Two thermometers measuring the water temperature exiting the heat exchangers are also used.

The helium gas used in the measurements is the same as used to pump balloons. Information about the gas is showed in table 4.8. A limitation in the design is that there is no possibility to measure the acceleration of the loudspeaker membrane, which is due to cost. With the acceleration it would be possible to determine the electroacoustic efficiency of the loudspeaker. So we are limited to look at the drive ratio which is the ratio between the oscillating pressure and the static pressure. A sketch of the final prototype is shown in figure 4.7.

ID number	UN1046
CAS number	744059-7
Molecular weight	4.0026
Specific volume	96.02 ft <sup>3</sup> /lb

Table 4.8: Information of the helium gas used in the measurements.

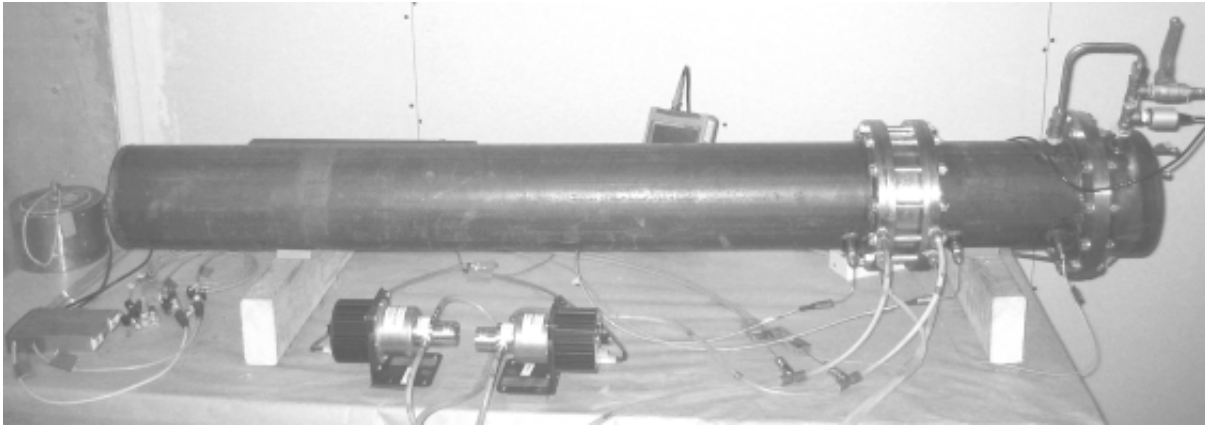


Figure 4.6: Picture of the final thermoacoustic heat pump prototype.

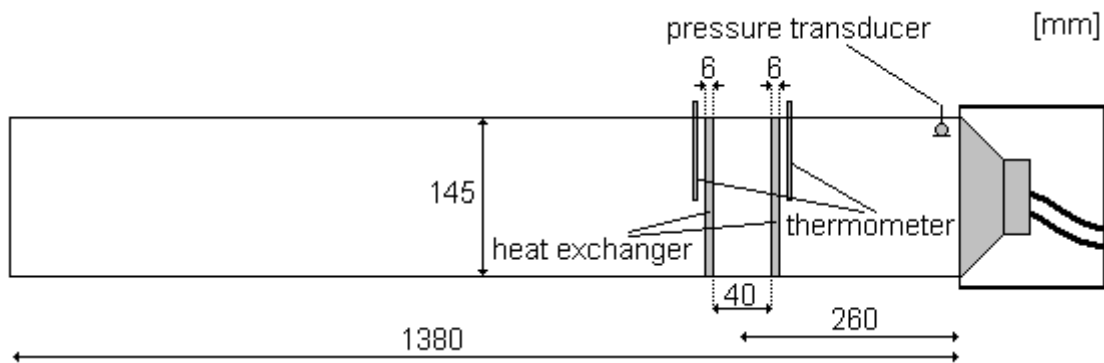


Figure 4.7: Sketch of the final thermoacoustic heat pump prototype. These are the final dimensions of the prototype.

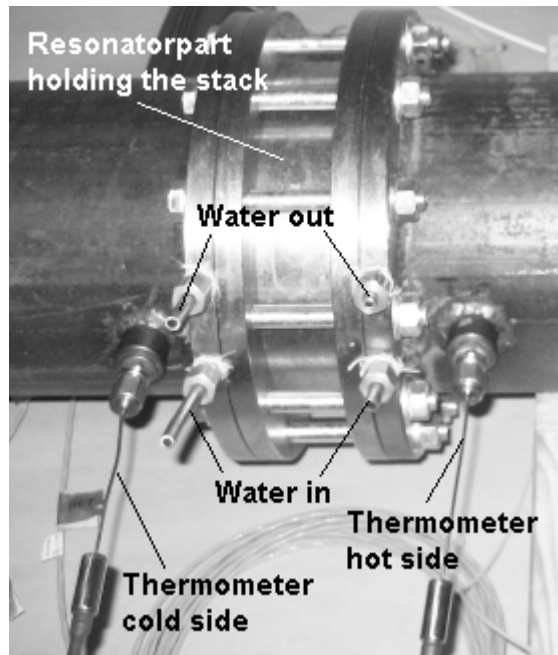


Figure 4.8: Close-up of the resonator part holding the stack. On each side of the stack a thermometer is mounted through the resonator wall to measure the temperature inside. It also shows where the water enters and exits the heat exchangers.

## Equipment

The equipment used during the measurements is summarized below.

- Amplifier - Yamaha M-35
- Loudspeaker - Beyma 6B10
- Pressure transducer - Dytran 2200V1
- Thermometer x4 - Thermocouple Type K
- Transmitter - PR electronics 5114A
- Water pump x2 - Micropump G150
- Manometer - FLUKE PV350
- Multimeter - FLUKE 8060

# 5 Measurements

The measurements will focus on a comparison between the resonator pressurized with helium and air at different levels of the static pressure. At every static pressure level the input power is varied to observe the temperature difference inside the resonator and the water exiting the heat exchangers. By comparing these two temperature differences the efficiency of the heat exchangers can be determined. The system is assumed to give the same temperature difference independent of the temperature entering the heat exchangers. For simplicity the velocity of the water is kept constant for all measurements.

## 5.1 Calibration

The pressure transducer, thermometers and water pumps are calibrated to ensure accurate output reading.

### 5.1.1 Pressure transducer

A small excitation current of 4mA is sent from the VXI-station through the BNC-cable. This is set in the Trigger Happy software, by setting the function to IEPE and AC-voltage. The sensitivity of the pressure transducer is 49.11mV/psi (pounds per square inch) where

$$1\text{psi} = 6.894760\text{kPa}$$

This results in a calibration factor used in the post processing of the measurement data.

$$cal_{transducer} = \frac{6.895\text{kPa}}{49.11\text{mV}} \approx 140\text{Pa/mV}$$

### 5.1.2 Thermometers

The calibration of the thermometers is performed by measuring the temperature of the water in a water tank and comparing the results with a reference thermometer. The reference thermometer is later used to measure the temperature of the water entering the heat exchangers. The output from the thermometers is recorded over a period of two minutes and a mean value is used to calculate a calibration factor used



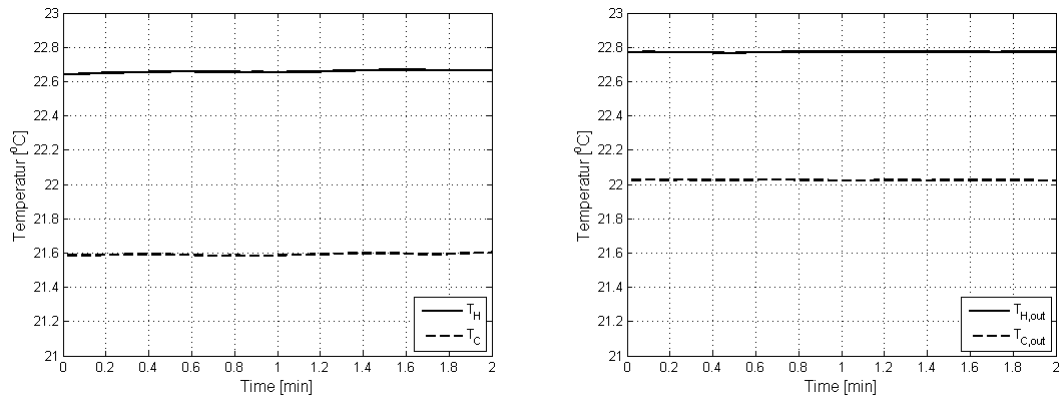


Figure 5.1: The results of the thermometer calibration, during which the reference thermometer displayed a temperature of  $T_{ref}=19.1^{\circ}\text{C}$ . The figure to the left shows the thermometers located inside the resonator and on the figure to the right shows the thermometers located where the water exits the heat exchangers. A mean value of the data is compared to the reference temperature, which results in a calibration factor for each thermometer used in the post processing of the measurement data.

in the post processing of the measurement data. The results for each thermometer are displayed in figure 5.1, during which the reference thermometer displayed a temperature of  $T_{ref}=19.1^{\circ}\text{C}$ . The thermometers measuring the hot temperature (subscript  $T_H$  and  $T_{H,out}$ ) are always connected to channel  $T_2$  and the thermometers measuring the cold temperatures ( $T_C$  and  $T_{C,out}$ ) is always connected to channel  $T_1$ , see figure 5.2.

### 5.1.3 Water pumps

Both water pumps are calibrated to determine the volume flow rate of the water circulating in the heat exchangers. A glass tank is filled with water to a level of above 1500ml. Both water pumps are adjusted to the lowest possible flow and where they have equal flow. The setting is marked on both water pumps and these settings will be the used for all measurement. Before the calibration starts the water pump is kept running for a while to reach a stable flow. The calibration process is started and when the water level in the glass tank reach 1500ml the time is started and a split time is recorded for every 250ml of water drained. The split times and the resulting volume flow rate  $U$  are shown in table 5.1. The calibration is performed for both water pumps.

	Pump 1	Pump 2
$t_{250}$	47.7s	50.1s
$t_{500}$	50.7s	51.8s
$t_{750}$	52.8s	52.7s
$t_{1000}$	56.4s	50.8s
$U$	$4.82 \cdot 10^{-6} \text{m}^3/\text{s}$	$4.87 \cdot 10^{-6} \text{m}^3/\text{s}$

Table 5.1: The results of the water pump calibration. The split times for every 250ml of water drained and the resulting volume flow rate  $U$  for each water pump.

## 5.2 Procedure

The measured data is acquired and recorded via a VXI-station using the Trigger Happy 4.0 software. The heat pump reaches stable conditions faster when the system is decreased from a higher to lower input power. So, the measurement is started at the highest used input power and is then decreased for each measurement. The frequency response of the resonator is first measured to ensure correct operating frequency. The voltage applied to the loudspeaker is calculated from a desired input power.

$$V_{IN} = \sqrt{W_{IN} R_L} \quad (5.1)$$

The impedance of the loudspeaker is measured with no load across the inputs with a multimeter to  $R_L=6\Omega$ . The water circulating in the heat exchangers is taken from a tank with the settings from the calibration and is collected in the same tank again. The location of the thermometers measuring the temperature of the water exiting the heat exchangers is at a distance 25cm from where the water exits the resonator. The temperature of the water in the tank that is entering the heat exchangers is assumed to be kept at a steady temperature through out a single measurement, but is checked and recorded before every measurement with the reference thermometer used in the calibration. The transmitter only holds to inputs ( $T_1$  and  $T_2$ ). For this reason the thermometers  $T_H$  and  $T_C$  (inside the resonator) are first recorded and then shifted to

$W_{IN}$	$V_{IN}$
20W	10.95V
30W	13.42V
40W	15.49V
50W	17.32V
60W	18.97V

Table 5.2: The input voltage to the loudspeaker calculated from a desired input power.

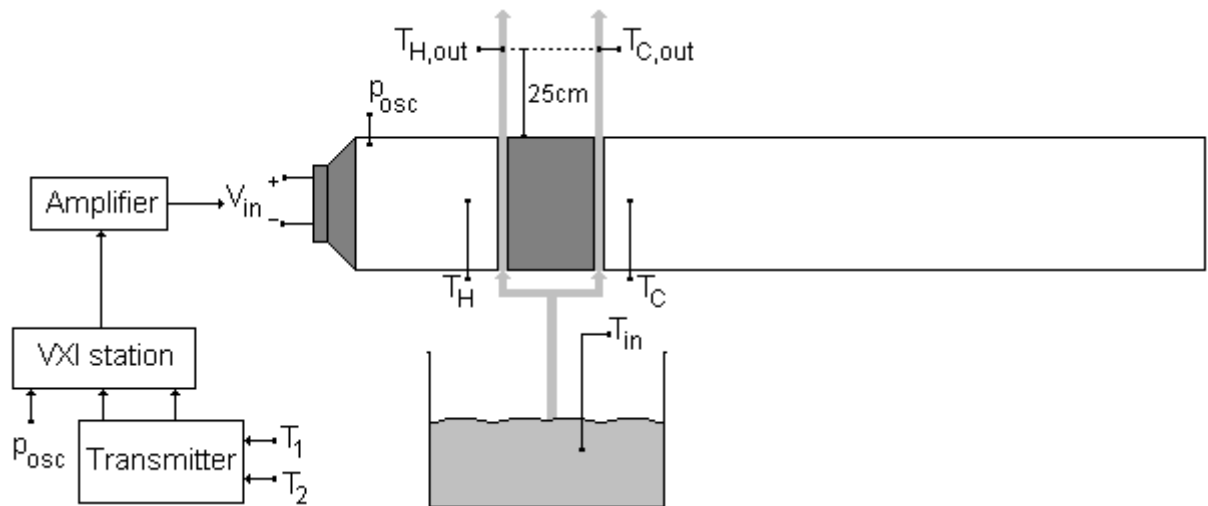


Figure 5.2: The scheme of the measurement set-up. First the thermometers inside the resonator is connected to the transmitter,  $T_H$  to  $T_2$  and  $T_C$  to  $T_1$ . The system is kept running and the thermometers measuring the water temperature is connected to the transmitter,  $T_{H,out}$  to  $T_2$  and  $T_{C,out}$  to  $T_1$ .

$T_{H,out}$  and  $T_{C,out}$  (water exiting the heat exchangers). A new measurement is started when the shift is done. A scheme of the measurement is illustrated in figure 5.2.

## 5.3 Results

The results from the measurements are presented as a temperature difference between the temperature on the hot and the cold side of the stack and the temperature between the water out of the hot and cold heat exchanger. All measurement results are included in appendix A.2.

### 5.3.1 Resonance

The resonance is measured before every set of measurements at a specific static pressure. Figure 5.3 shows the frequency spectrum of the resonator at 400kPa static pressure. The resonance just above 100Hz correspond to the fundamental frequency of the resonator. The lower graph shows the peak of the resonance magnified to determine the operating frequency. This was set to 115Hz. The resonance is the same at all static pressure, with an exception at 1bar where the resonance was slightly higher at 118Hz. This frequency was used in the measurements at 1bar.

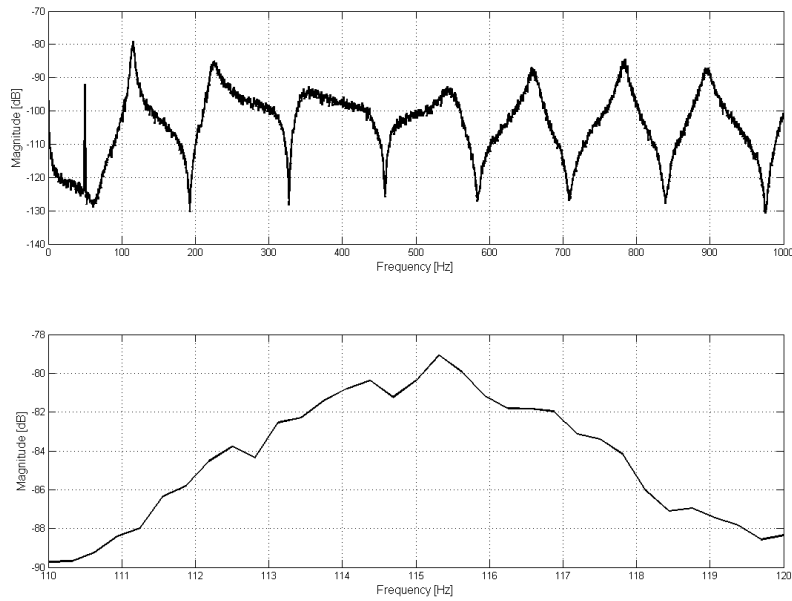


Figure 5.3: The measured resonance with air at a static pressure of 400kPa. The lower graph shows the fundamental frequency of the resonator magnified to determine the operating frequency. This was set to  $f=115\text{Hz}$ .

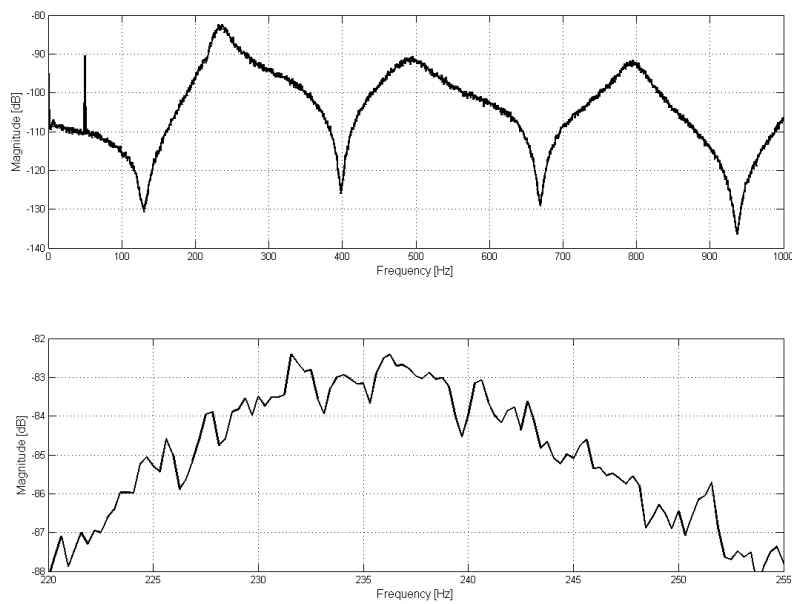


Figure 5.4: The measured resonance with helium at a static pressure of 400kPa. The lower graph shows the fundamental frequency of the resonator magnified to determine the operating frequency. This was set to  $f=236\text{Hz}$ .

Figure 5.4 shows the frequency spectrum with helium as working gas. It was not possible to completely fill the heat pump with helium, due to a problem in the construction. The lower graph again shows the peak of the resonance magnified corresponding to the fundamental frequency of the resonator and the operating frequency was chosen to 236Hz. The ideal operating frequency would be close to 370Hz.

### 5.3.2 Temperature difference depending on input power

The input power is varied to compare the temperature differences between the hot and cold sides in the resonator and the cold and hot water at different mean static pressure. Figure 5.5 shows the resulting temperature differences driven at 100kPa and 200kPa and with a input power of 20W and 30W. With increasing static pressure and input power it is possible to observe a small increase in the output temperature difference as well as the temperature difference inside the resonator. Comparing the top left graph ( $p_m=100\text{kPa}$ ,  $W_{IN}=20\text{W}$ ) the bottom right ( $p_m=200\text{kPa}$ ,  $W_{IN}=30\text{W}$ ) it is clear the output temperature difference has increased. The desired temperature difference inside would be around  $4^\circ\text{C}$  to achieve  $\Gamma \approx 1/3$ . Figure 5.6 shows the results at static pressure 400kPa and input power of 40W, 50W and 60W. Now we can observe that the temperature difference inside the has approached  $4^\circ\text{C}$ . This should mean that the desired value of the operation parameter  $\Gamma \approx 1/3$  is achieved. Still we are not able to extract all of the heat inside the heat pump.

### 5.3.3 Helium

We were able to raise the resonance from 115Hz to 236Hz by filling the resonator with helium. It was not investigated how much helium we were able to fill, but we should be able to observe a difference in the behavior. We can observe an output temperature difference in figure 5.7 that is close to the previous results in figure 5.6. The temperature difference inside is lower and shows strange behavior in the results with  $W_{IN}=30\text{W}$ . The temperature difference should be above  $4^\circ\text{C}$  to achieve  $\Gamma \approx 1/3$ . Using the heat pump with helium needs to be investigated further.

### 5.3.4 Drive ratio

The calculated total and acoustic power in section 4.3.1 used a drive ratio of  $D=0.05$ . In practical situations this can be regarded as high and difficult to achieve with an unmodified hifi loudspeaker.

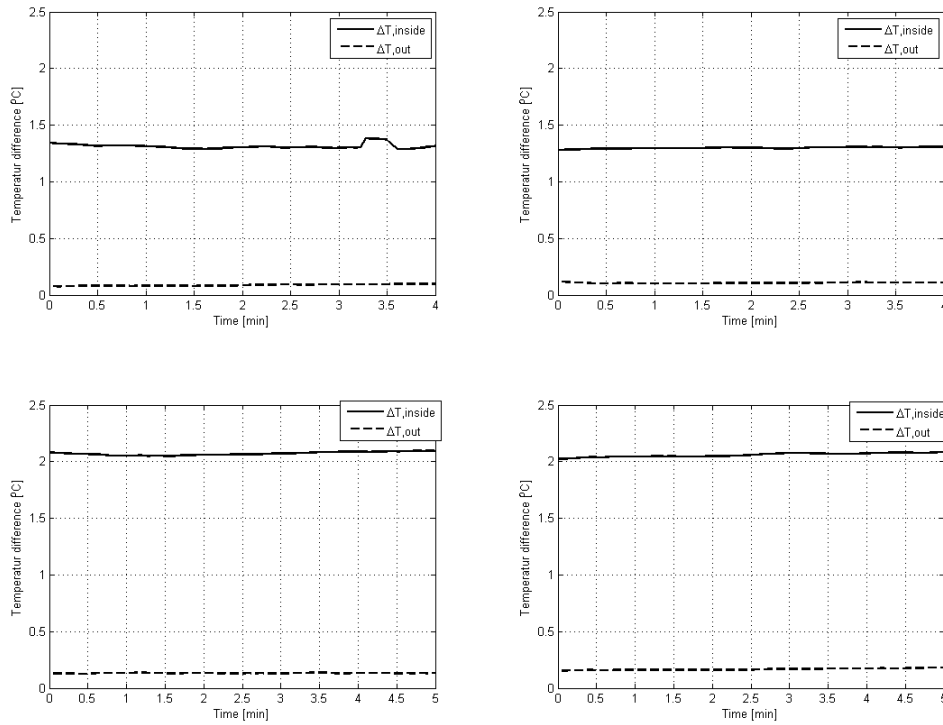


Figure 5.5: The measured temperature differences with air. The graphs at the top are measured with a static pressure of 100kPa and the graphs at the bottom is measured with a static pressure of 200kPa. The graphs to the left have an input power of 20W and the graphs to the right have an input power of 30W.

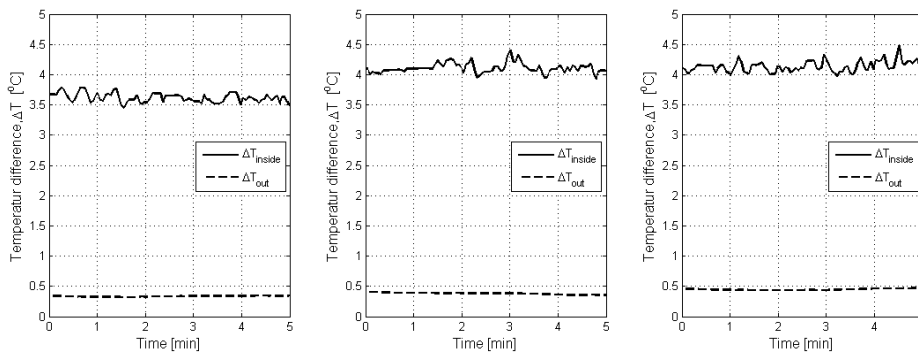


Figure 5.6: The measured temperature differences with air and static pressure at 400kPa. The graph to the left is measured with an input power of 40W, the graph in the middle with an input power of 50W and the graph to the right an input power of 60W.

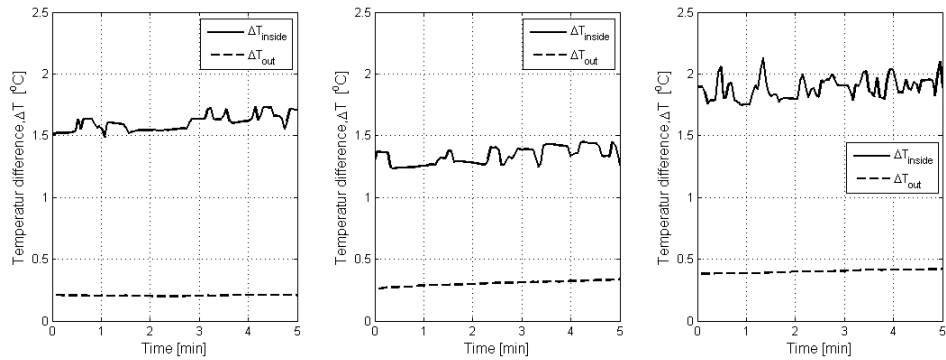


Figure 5.7: The measured temperature difference with helium and static pressure at 400kPa. The graph to the left is measured with an input power of 20W, the graph in the middle with an input power of 30W and the graph to the right an input power of 40W.

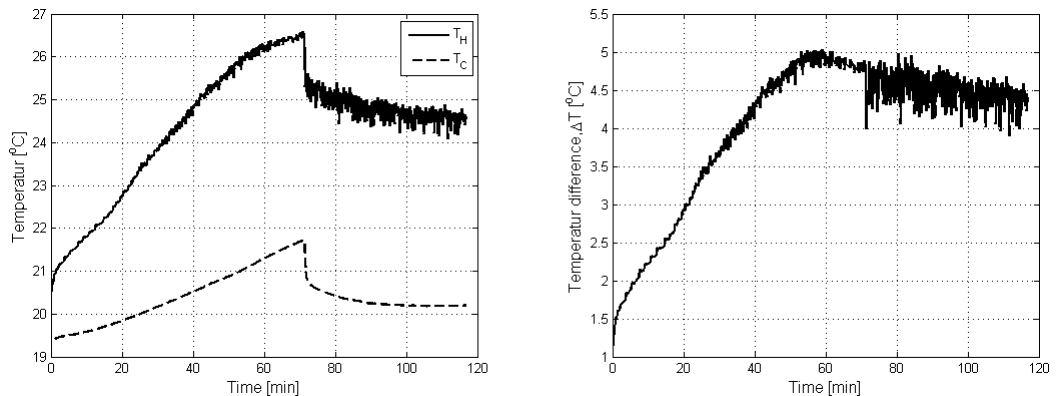


Figure 5.8: The graph to the left shows temperature of the both sides of the stack. After about 70 minutes the heat exchangers are turned on to observe if they have any effect. The graph to the right shows the temperature difference between the hot and cold side of the stack. The thermometer on the right side shows some strange behavior with variations in temperature which cannot be explained.

Table 5.3 shows the measured drive ratios for all measurements. It shows that the drive ratio is low compared to the value used in the calculations. The drive ratio decreases slightly with increasing static pressure and for helium the drive ratio is lower for the same input power compared to air. The drive ratio for air at 400kPa

	Air 100kPa	Air 200kPa	Air 300kPa	Air 400kPa	Helium 400kPa
20W	0.69%	0.54%	0.50%	0.47%	0.28%
30W	0.83%	0.65%	0.59%	0.55%	0.34%
40W	-	-	-	0.61%	0.38%
50W	-	-	-	0.67%	-
60W	-	-	-	0.72%	-

Table 5.3: The measured drive ratio for all measurements.

was measured up to 60W. Still the drive ratio is below 1%, so the driver needs to be improved to reach a high drive ratio and higher power. Table 5.4 shows the difference in power between the highest achieved drive ratio of 0.72% at 400kPa and a drive ratio of 5%. The results is calculated with a DeltaE model of the final prototype included in appendix A.1. It is clear that there is a big difference in the results, but still the measurement set-up suffers from low efficiency of the heat exchangers.

	$D=0.72\%$	$D=5\%$
$H$	0.8W	34W
$\Delta W$	0.5W	21W
$Q_H$	1.5W	62W

Table 5.4: Comparison between the highest measured drive ratio of  $D=0.72\%$  and a drive ratio of  $D=5\%$ . The results are calculated with DeltaE and the dimensions of the measurement set-up.

### 5.3.5 Efficiency of heat exchangers

Figure 5.8 shows the effect of the heat exchangers. The graph to the left shows the heat pump is started and kept running without the water in the heat exchangers running and after about 70min the water is turned on. In the graph to the right we can see that the temperature difference increases to a point where it stabilizes and evens out. When the heat exchangers are turned on the temperature shifts down, although the temperature difference stays stable. The efficiency of the heat exchangers in table 5.5



is determined by,

$$HX_{eff} = \frac{\Delta T_{out}}{\Delta T_{inside}} \quad (5.2)$$

where  $\Delta T_{out}$  is the temperature difference of the water exiting the heat exchangers and  $\Delta T_{inside}$  is the temperature difference between the hot and cold side of the stack. The results differs between the measurements and conditions. This makes it hard to interpret and compare the results. Taking a mean value of all the results in table 5.5 gives an efficiency of around 12%.

	Air 100kPa	Air 200kPa	Air 300kPa	Air 400kPa	Helium 400kPa
20W	6.6%	6.4%	15.5%	12.3%	12.8%
30W	8.2%	8.1%	15.2%	12.2%	23.0%
40W	-	-	-	9.3%	21.3%
50W	-	-	-	9.2%	-
60W	-	-	-	10.8%	-

Table 5.5: The measured efficiency of the heat exchangers determined as a ratio between the output temperature difference and the inside temperature difference.

To calculate the rate at which heat is extracted from the heat exchanger at the hot side we can use the temperature difference between the water entering and exiting the heat exchanger. The heat  $Q$  can be obtained [2] from

$$Q = \rho c_p (T_{out} - T_{in}) U \quad (5.3)$$

where  $\rho$  is the fluids density,  $c_p$  is the fluids specific heat capacity and  $U$  is the volume flow rate of the fluid in the heat exchanger. The volume flow rate has been determined during the calibration of the water pumps and is taken from table 5.1. The density of water is around  $\rho_w=1000\text{kg/m}^3$  and the specific heat is around  $c_p=4200\text{J/kgK}$ . Table 5.6 shows the heat extracted for different  $\Delta T$  between the water entering and exiting the hot heat exchanger. The measured temperature difference between the water entering and exiting the hot heat exchanger is below  $\Delta T=0.1$  and cannot be determined exactly due the sensitivity of the reference thermometer.

	$\Delta T=0.1^\circ\text{C}$	$\Delta T=0.2^\circ\text{C}$	$\Delta T=0.3^\circ\text{C}$	$\Delta T=0.4^\circ\text{C}$	$\Delta T=0.5^\circ\text{C}$
Q	2.1W	4.1W	6.2W	8.2W	10.3W

Table 5.6: The heat calculated with increasing  $\Delta T$  between the water entering and exiting the hot heat exchanger.

## 6 Discussion and conclusion

A thermoacoustic heat pump was designed to reach a desired net power contribution of  $\Delta W_{HP} \approx 250W$  to increase the energy efficiency of a tumble dryer. The design choices involved difficult construction issues like high static pressure and use of helium inside the heat pump. The prototype developed in this thesis suffers from low electroacoustic efficiency in the driver and low efficiency of heat transfer in the heat exchangers and we were not able to reach the desired performance. There are no standard solutions concerning design of high efficient drivers and heat exchangers. This prototype gives a good grounding for further development. For satisfactory agreement between the calculations and measurement results the issue of efficiency has to be solved.

With an increase in static pressure there is an improvement in performance, which was showed in the calculations and measurement results. The heat pump was designed to hold a static pressure of up to 4bar, which in the calculations was enough to reach the desired net power contribution. A drawback is that the calculations assume a high efficient driver and heat exchangers.

It was shown that an increase in drive ratio increases the power substantially, but at very high drive ratios nonlinear effects can arise. A driver ratio of  $D=5\%$  was used in the calculations to reach the desired power. A drive ratio of  $D=5\%$  is not a limit but can be seen as an aim in further development. The highest achieved drive ratio at  $p_m=400kPa$  was  $D=0.72\%$  which was reached with input power  $W_{IN}=60W$ .

Operating the heat pump with helium resulted in a lower drive ratio compared to air with the same input power. Therefore, achieving equal drive ratios would require higher input power with helium. We were not able to completely fill the heat pump with helium, due to a problem in the design. This issue has to be solved to perform further measurements with helium.

### 6.1 Future work

There are two important issues to be addressed in future work. It would be good to look separately at the driver and the heat exchangers.

The driver can be optimized to reach optimal electroacoustic efficiency. This would be done by matching the mechanical resonance of the driver to the acoustical reso-

nance of the resonator. This can be made by modifying the loudspeaker, for example by increasing the stiffness of the membrane. It would be interesting to add an accelerometer inside the heat pump to determine the acoustic power.

The heat exchangers can be optimized to have optimal length and area. The area can be increased by adding more rotations in the spiral construction and a thinner copper tube. The volume flow rate of the water can also be examined and optimized.

When the issues of driver and heat exchanger efficiency is solved, the dimensions of the stack or rather the channel geometry in the stack can be evaluated for further optimization of the performance. In the final stages the dimensions of the heat pump to fit it inside the tumble dryer can also be investigated. A real application inside a tumble dryer is at this point far away, but with high class engineering work it should be possible to reach.

# References

## Literature

- [1] Swift, G. W., *Thermoacoustics engines*, J. Acoust. Soc. Am. 84 (4), 1145-1180, 1988
- [2] Swift, G. W., *Thermoacoustics: A unifying perspective for some engines and refrigerators*, Acoustical Society of America, 2002
- [3] Andersson, P. B. U., *Review of Thermoacoustic Refrigeration. Description of a Simple Thermoacoustic Refrigerator for Demonstration Purpose*, Thesis work, Department of Applied Acoustics, Chalmers University of Technology, Göteborg, 1999
- [4] Tijani, M. E. H., *Loudspeaker-driven thermoacoustic refrigeration*, Ph.D. dissertation, Applied Physics Department, Technical University at Eindhoven, 2001
- [5] Ward, B., Swift, G., *Design Environment for Low-amplitude ThermoAcoustic Engines, Version 5.4*, Tutorial and User's Guide, Los Alamos National Laboratory, 2004
- [6] Liu, J., Garret, S. L., Long, S. L., Sen, A., *Seperation of thermoviscous losses in Celcor<sup>TM</sup> ceramic*, J. Acoust. Soc. Am. 119 (2), 857-862, 2006
- [7] Ahlborn, B., Camire J., *Thermoacoustic heat pumps with maximum power transfer*, Am. J. Phys. 63 (5), 449-451, 1994
- [8] Swedish Energy Agency, *STEMFS 2005:6, Statens energimyndighets föreskrift om information om energiförbrukning hos elektriska torktumlare för hushållsbruk*

## Internet pages

- [9] <http://en.wikipedia.org/wiki/Thermoacoustics> Wikipedia - The Free Encyclopedia
- [10] <http://www.lanl.gov/thermoacoustics/> Los Alamos National Laboratory
- [11] [http://www.benjerry.com/our\\_company/sounds\\_cool/](http://www.benjerry.com/our_company/sounds_cool/) Ben & Jerry's, Sounds Cool!, Adventures in Thermoacoustic Refrigeration!

# A Appendix

## A.1 DeltaE Programs

```

TITLE      Thermoacoustic heat pump, parallel stack, D = 5%
!->paraD5.out
!Created@14:35:02 23-Mar-07 with DeltaE Vers. 5.5b6 for the IBM/PC-Compatible
!----- 0 -----
BEGIN
4.0000E+05 a Mean P      Pa          397.40    A Freq.  G( 0b)    P
 397.40    b Freq.      Hz          309.16    B T-beg  G( 0c)    P
 309.16    c T-beg     K           1.5157E-02 C |U|    G( 0f)    P
2.0000E+04 d |p|       Pa          -382.36   D HeatIn G( 3e)    P
 0.0000    e Ph(p)     deg          236.67   E HeatIn G( 6e)    P
1.5157E-02 f |U|      m^3/s      G
 0.0000    g Ph(U)     deg
helium     Gas type
ideal      Solid type
!----- 1 -----
ENDCAP
1.7000E-02 a Area       m^2          2.0000E+04 A |p|      Pa
              0.0000    B Ph(p)      deg
              1.5074E-02 C |U|      m^3/s
              0.0000    D Ph(U)      deg
              150.74    E Hdot       W
sameas      0 Gas type
              150.74    F Edot       W
ideal       Solid type
              -0.8338   G HeatIn    W
!----- 2 -----
DUCT
sameas      1a a Area    m^2          1.7286E+04 A |p|      Pa
 0.4618    b Perim     m           -0.9180   B Ph(p)    deg
 0.2180    c Length    m           0.2657    C |U|      m^3/s
              -87.280    D Ph(U)    deg
              145.70    E Hdot       W
sameas      0 Gas type
              145.70    F Edot       W
ideal       Solid type
              -5.0460   G HeatIn    W

```

```

!----- 3 -----
HX          Hot HX
sameas 1a a Area      m^2      1.6725E+04 A |p|      Pa
          0.8583 b GasA/A          -0.6981 B Ph(p)      deg
1.6700E-02 c Length    m          0.2829 C |U|      m^3/s
5.4500E-04 d y0        m          -87.874 D Ph(U)      deg
-382.36 e HeatIn      W          G          -236.67 E Hdot      W
308.00 f Est-T        K          = 3H?      116.59 F Edot      W
sameas 0 Gas type          -382.36 G Heat      W
copper Solid type          308.00 H MetalT    K
!----- 4 -----
STKSLAB
sameas 1a a Area      m^2      1.5227E+04 A |p|      Pa
          0.8583 b GasA/A          2.7962E-02 B Ph(p)      deg
4.0000E-02 c Length    m          0.3209 C |U|      m^3/s
5.4500E-04 d y0        m          -88.682 D Ph(U)      deg
9.0000E-05 e Lplate    m          -236.67 E Hdot      W
          55.028 F Edot      W
          309.16 G T-beg      K
sameas 0 Gas type          299.34 H T-end      K
celcor Solid type          -61.561 I StkEdt     W
!----- 5 +++++ therm insul mode +++++
INSULATE
!----- 6 +++++ therm insul mode +++++
HX          Cold HX
sameas 1a a Area      m^2      1.4538E+04 A |p|      Pa
sameas 3b b GasA/A          0.4303 B Ph(p)      deg
sameas 3c c Length    m          0.3361 C |U|      m^3/s
sameas 3d d y0        m          -89.001 D Ph(U)      deg
236.67 e HeatIn      W          G          1.1369E-13 E Hdot     W
300.00 f Est-T        K          = 6H?      24.251 F Edot      W
sameas 0 Gas type          236.67 G Heat      W
copper Solid type          300.00 H MetalT    K
!----- 7 +++++ therm insul mode +++++
DUCT
sameas 1a a Area      m^2      1.9468E+04 A |p|      Pa
sameas 2b b Perim      m          -179.32 B Ph(p)      deg
          0.9823 c Length    m          7.8940E-05 C |U|      m^3/s
          -179.32 D Ph(U)      deg
sameas 0 Gas type          1.1369E-13 E Hdot     W
ideal Solid type          0.7684 F Edot      W
!----- 8 +++++ therm insul mode +++++

```

```

ENDCAP
sameas 1a a Area      m^2          1.9468E+04 A |p|      Pa
                                     -179.32  B Ph(p)    deg
                                     8.8083E-17 C |U|    m^3/s
                                     -84.003  D Ph(U)    deg
sameas 0 Gas type          1.1369E-13 E Hdot    W
ideal   Solid type        -7.9499E-14 F Edot   W
!----- 9 +++++ therm insul mode +++++

```

```

HARDEND
0.0000 a R(1/z)          = 9G?    1.9468E+04 A |p|      Pa
0.0000 b I(1/z)          = 9H?    -179.32  B Ph(p)    deg
0.0000 c Hdot      W     = 9E?    8.8083E-17 C |U|    m^3/s
                                     -84.003  D Ph(U)    deg
                                     1.1369E-13 E Hdot    W
                                     -7.9499E-14 F Edot   W
                                     -1.6160E-17 G R(1/z)
sameas 0 Gas type          1.7354E-16 H I(1/z)
ideal   Solid type        299.34   I T      K

```

```

! The restart information below was generated by a previous run
! You may wish to delete this information before starting a run
! where you will (interactively) specify a different iteration
! mode. Edit this table only if you really know your model!

```

```

guessz 0b 0c 0f 3e 6e
xprecn 3.0481E-03 -3.5189E-04 4.9579E-07 -2.9090E-03 -2.2964E-03
hilite 3e 4I 6e
targs 3f 6f 9a 9b 9c
SPECIALS 0

```



```

TITLE      Thermoacoustic heat pump, rectangular stack, D = 5%
!->rectD5.out
!Created@18:30:03 28-Mar-07 with DeltaE Vers. 5.5b6 for the IBM/PC-Compatible
!----- 0 -----
BEGIN
  4.0000E+05 a Mean P      Pa              396.12    A Freq.  G( 0b)    P
    396.12    b Freq.      Hz              310.63    B T-beg  G( 0c)    P
    310.63    c T-beg      K              1.6624E-02 C |U|    G( 0f)    P
  2.0000E+04 d |p|        Pa              -395.94   D HeatIn G( 3e)    P
    0.0000    e Ph(p)      deg              235.73   E HeatIn G( 6e)    P
  1.6624E-02 f |U|        m^3/s        G
    0.0000    g Ph(U)      deg
helium      Gas type
ideal       Solid type
!----- 1 -----
ENDCAP
  1.7000E-02 a Area        m^2              2.0000E+04 A |p|      Pa
    0.0000    B Ph(p)      deg
    1.6541E-02 C |U|      m^3/s
    0.0000    D Ph(U)      deg
    165.41    E Hdot        W
sameas     0 Gas type
ideal      Solid type
    165.41    F Edot        W
    -0.8358   G HeatIn      W
!----- 2 -----
DUCT
sameas     1a a Area        m^2              1.7170E+04 A |p|      Pa
    0.4618    b Perim      m              -1.0341   B Ph(p)    deg
    0.2240    c Length     m              0.2716    C |U|      m^3/s
    -87.094   D Ph(U)      deg
    160.20    E Hdot        W
sameas     0 Gas type
ideal      Solid type
    160.20    F Edot        W
    -5.2030   G HeatIn      W
!----- 3 -----
HX          Hot HX
sameas     1a a Area        m^2              1.6937E+04 A |p|      Pa
    0.7366    b GasA/A      deg              -0.9500   B Ph(p)    deg
  6.0000E-03 c Length     m              0.2769    C |U|      m^3/s
  5.4500E-04 d y0         m              -87.289   D Ph(U)    deg
 -395.94    e HeatIn      W          G          -235.73   E Hdot      W
  307.00    f Est-T       K          = 3H?      149.74    F Edot      W
sameas     0 Gas type
copper     Solid type
    -395.94   G Heat        W
    307.00    H MetalT     K

```

```

!----- 4 -----
STKRECT
sameas 1a a Area      m^2      1.5030E+04 A |p|      Pa
      0.7366 b GasA/A      1.0627 B Ph(p)      deg
4.0000E-02 c Length  m      0.3112 C |U|      m^3/s
5.4500E-04 d a      m      -88.092 D Ph(U)      deg
9.0000E-05 e Lplate  m      -235.73 E Hdot      W
5.4500E-04 f b      m      34.511 F Edot      W
      310.63 G T-beg      K
sameas 0 Gas type      297.85 H T-end      K
celcor Solid type      -115.23 I StkEdt      W
!----- 5 +++++ therm insul mode +++++
INSULATE
!----- 6 +++++ therm insul mode +++++
HX      Cold HX
sameas 1a a Area      m^2      1.4755E+04 A |p|      Pa
sameas 3b b GasA/A      1.2269 B Ph(p)      deg
sameas 3c c Length  m      0.3159 C |U|      m^3/s
sameas 3d d y0      m      -88.191 D Ph(U)      deg
      235.73 e HeatIn  W      G      2.1648E-09 E Hdot      W
      300.00 f Est-T  K      = 6H?      23.666 F Edot      W
sameas 0 Gas type      235.73 G Heat      W
copper Solid type      300.00 H MetalT      K
!----- 7 +++++ therm insul mode +++++
DUCT
sameas 1a a Area      m^2      1.9146E+04 A |p|      Pa
sameas 2b b Perim  m      -178.54 B Ph(p)      deg
      0.9980 c Length  m      7.7177E-05 C |U|      m^3/s
      -178.54 D Ph(U)      deg
sameas 0 Gas type      2.1648E-09 E Hdot      W
ideal Solid type      0.7388 F Edot      W
!----- 8 +++++ therm insul mode +++++
ENDCAP
sameas 1a a Area      m^2      1.9146E+04 A |p|      Pa
      -178.54 B Ph(p)      deg
      4.9774E-10 C |U|      m^3/s
      85.624 D Ph(U)      deg
sameas 0 Gas type      2.1648E-09 E Hdot      W
ideal Solid type      -4.8439E-07 F Edot      W
!----- 9 +++++ therm insul mode +++++
HARDEND
      0.0000 a R(1/z)      = 9G?      1.9146E+04 A |p|      Pa

```

0.0000	b	I(1/z)	=	9H?	-178.54	B Ph(p)	deg
0.0000	c	Hdot	W	=	9E?	4.9774E-10	C  U  m <sup>3</sup> /s
					85.624	D Ph(U)	deg
					2.1648E-09	E Hdot	W
					-4.8439E-07	F Edot	W
					-1.0206E-10	G R(1/z)	
sameas	0	Gas type			-9.9875E-10	H I(1/z)	
ideal		Solid type			297.85	I T	K

! The restart information below was generated by a previous run  
! You may wish to delete this information before starting a run  
! where you will (interactively) specify a different iteration  
! mode. Edit this table only if you really know your model!

guessz	0b	0c	0f	3e	6e		
xprecn	-4.8556E-03	2.2715E-04	1.3287E-07	3.4419E-03	3.9812E-03		
hilite	3e	4I	6e				
targs	3f	6f	9a	9b	9c		
SPECIALS	0						

TITLE Thermoacoustic heat pump, Model of the final prototype, p\_m=400Kpa D=0.72%  
 !->rect.out

!Created@09:45:53 29-Mar-07 with DeltaE Vers. 5.5b6 for the IBM/PC-Compatible

!----- 0 -----

BEGIN

4.0000E+05	a	Mean P	Pa		124.35	A	Freq.	G( 0b)	P
124.35	b	Freq.	Hz	G	299.15	B	T-beg	G( 0c)	P
299.15	c	T-beg	K	G	4.4505E-04	C	U	G( 0f)	P
2880.0	d	p	Pa		-1.4529	D	HeatIn	G( 3e)	P
0.0000	e	Ph(p)	deg		0.8308	E	HeatIn	G( 6e)	P
4.4505E-04	f	U	m <sup>3</sup> /s	G					
0.0000	g	Ph(U)	deg						
air		Gas type							
ideal		Solid type							

!----- 1 -----

ENDCAP

1.7000E-02	a	Area	m <sup>2</sup>		2880.0	A	p	Pa	
					0.0000	B	Ph(p)	deg	
					4.4341E-04	C	U	m <sup>3</sup> /s	
					0.0000	D	Ph(U)	deg	
					0.6385	E	Hdot	W	
sameas	0	Gas type			0.6385	F	Edot	W	
ideal		Solid type			-2.3535E-03	G	HeatIn	W	

!----- 2 -----

DUCT

sameas	1a	a	Area	m <sup>2</sup>	2488.1	A	p	Pa	
					-0.4710	B	Ph(p)	deg	
					1.5266E-02	C	U	m <sup>3</sup> /s	
					-88.594	D	Ph(U)	deg	
					0.6221	E	Hdot	W	
sameas	0	Gas type			0.6221	F	Edot	W	
ideal		Solid type			-1.6420E-02	G	HeatIn	W	

!----- 3 -----

HX Hot HX

sameas	1a	a	Area	m <sup>2</sup>	2460.3	A	p	Pa	
					-0.4535	B	Ph(p)	deg	
					1.5537E-02	C	U	m <sup>3</sup> /s	
					-88.652	D	Ph(U)	deg	
					-0.8308	E	Hdot	W	
					0.6007	F	Edot	W	
sameas	0	Gas type			-1.4529	G	Heat	W	
copper		Solid type			299.00	H	MetalT	K	

```

!----- 4 -----
STKRECT
sameas 1a a Area      m^2      2232.5    A |p|      Pa
      0.7366 b GasA/A
4.0000E-02 c Length  m      1.7284E-02 C |U|      m^3/s
5.4500E-04 d      a      m      -89.071   D Ph(U)    deg
9.0000E-05 e Lplate  m      -0.8308   E Hdot     W
5.4500E-04 f      b      m      0.1309   F Edot     W
      299.15   G T-beg   K
sameas 0 Gas type    293.92   H T-end    K
celcor Solid type    -0.4699  I StkEdt   W
!----- 5 +++++ therm insul mode +++++
INSULATE
!----- 6 +++++ therm insul mode +++++
HX      Cold HX
sameas 1a a Area      m^2      2200.5    A |p|      Pa
sameas 3b b GasA/A
sameas 3c c Length  m      1.7526E-02 C |U|      m^3/s
sameas 3d d y0      m      -89.096   D Ph(U)    deg
      0.8308 e HeatIn  W      G      1.6663E-12 E Hdot     W
      294.00 f Est-T   K      = 6H?    0.1078   F Edot     W
sameas 0 Gas type    0.8308   G Heat     W
copper Solid type    294.00   H MetalT   K
!----- 7 +++++ therm insul mode +++++
DUCT
sameas 1a a Area      m^2      2768.7    A |p|      Pa
sameas 2b b Perim    m      -179.31   B Ph(p)    deg
      1.0940 c Length  m      1.5453E-06 C |U|      m^3/s
      -179.31   D Ph(U)    deg
sameas 0 Gas type    1.6663E-12 E Hdot     W
ideal Solid type     2.1393E-03 F Edot     W
!----- 8 +++++ therm insul mode +++++
ENDCAP
sameas 1a a Area      m^2      2768.7    A |p|      Pa
      -179.31   B Ph(p)    deg
      1.3949E-11 C |U|      m^3/s
      85.917   D Ph(U)    deg
sameas 0 Gas type    1.6663E-12 E Hdot     W
ideal Solid type     -1.6082E-09 F Edot     W
!----- 9 +++++ therm insul mode +++++
HARDEND
      0.0000 a R(1/z)      = 9G?    2768.7    A |p|      Pa

```

```

0.0000 b I(1/z)      = 9H?   -179.31   B Ph(p)   deg
0.0000 c Hdot      W   = 9E?   1.3949E-11 C |U|   m^3/s
                        85.917   D Ph(U)   deg
                        1.6663E-12 E Hdot   W
                        -1.6082E-09 F Edot   W
                        -4.0215E-11 G R(1/z)
sameas  0 Gas type    -4.8120E-10 H I(1/z)
ideal   Solid type    293.92   I T      K

```

```

! The restart information below was generated by a previous run
! You may wish to delete this information before starting a run
! where you will (interactively) specify a different iteration
! mode. Edit this table only if you really know your model!

```

```

guessz   0b 0c 0f 3e 6e
xprecn  -3.2151E-03  2.7340E-04 -7.4145E-10 -7.8853E-06  1.0947E-05
hilite   3e 4I 6e
targs    3f 6f 9a 9b 9c
SPECIALS  0

```

## A.2 Measurements

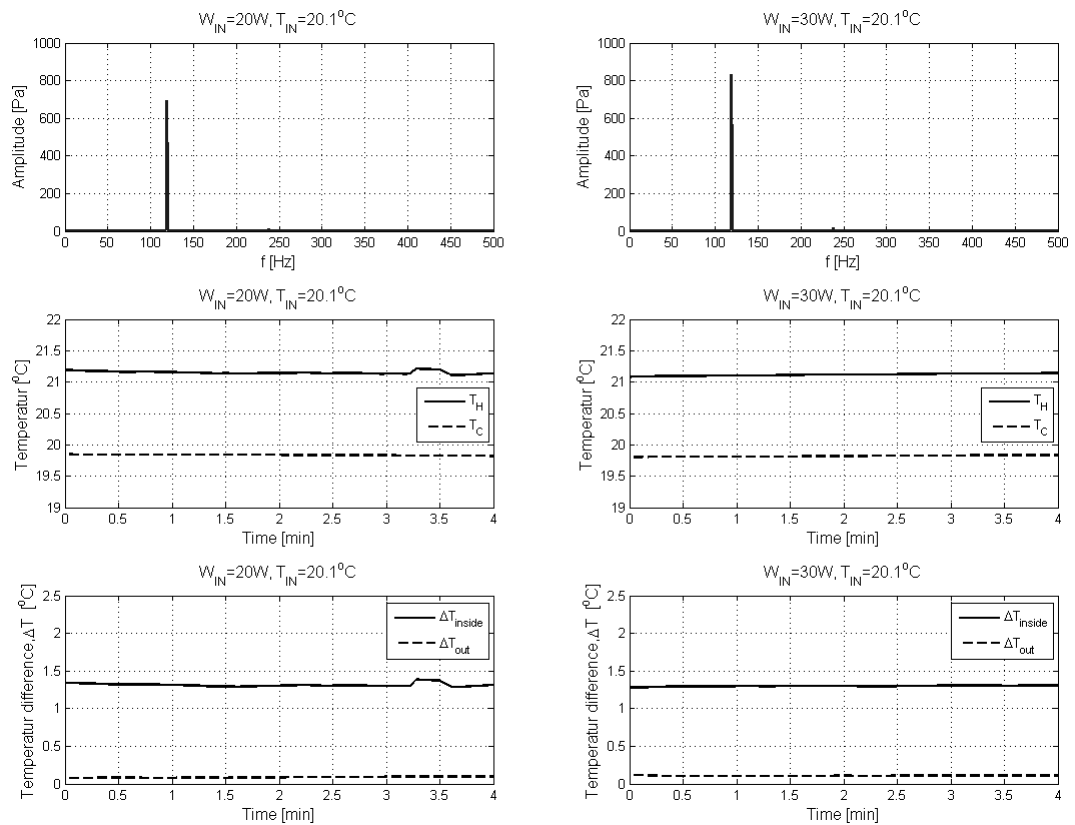


Figure A.1: Results from measurements with air, static pressure 100kPa and input power 20-30W.

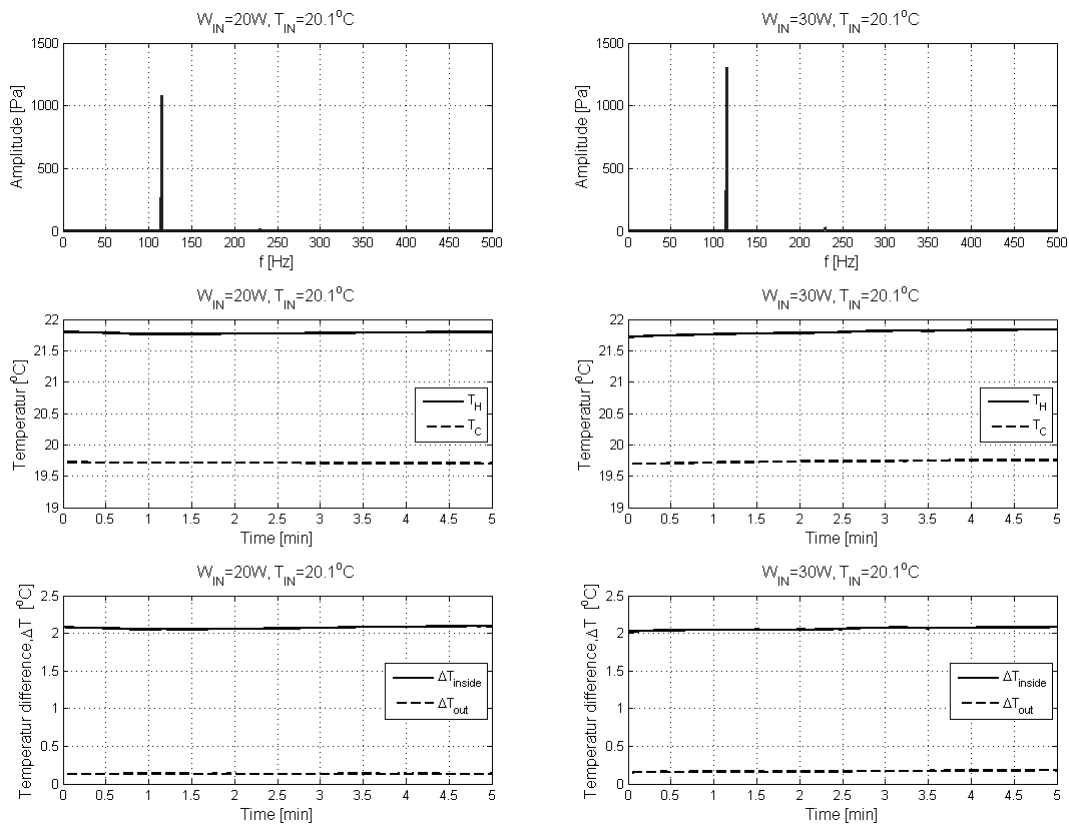


Figure A.2: Results from measurements with air, static pressure 200kPa and input power 20-30W.



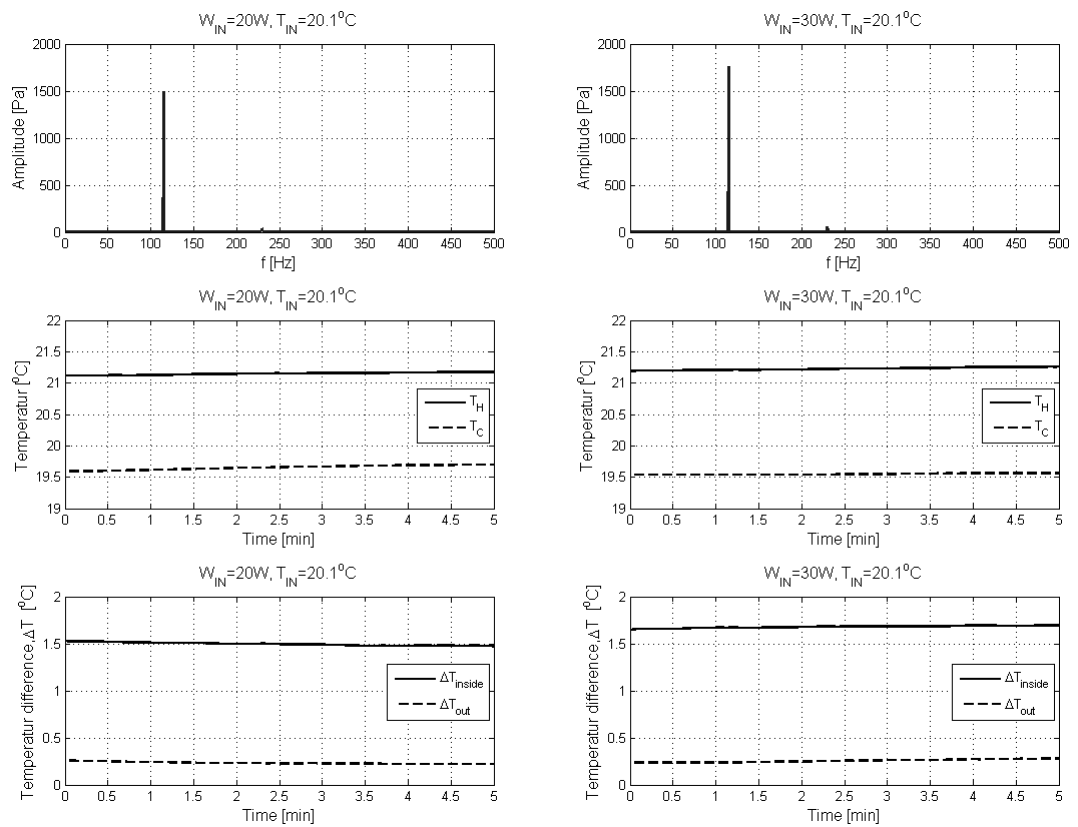


Figure A.3: Results from measurements with air, static pressure 300kPa and input power 20-30W.

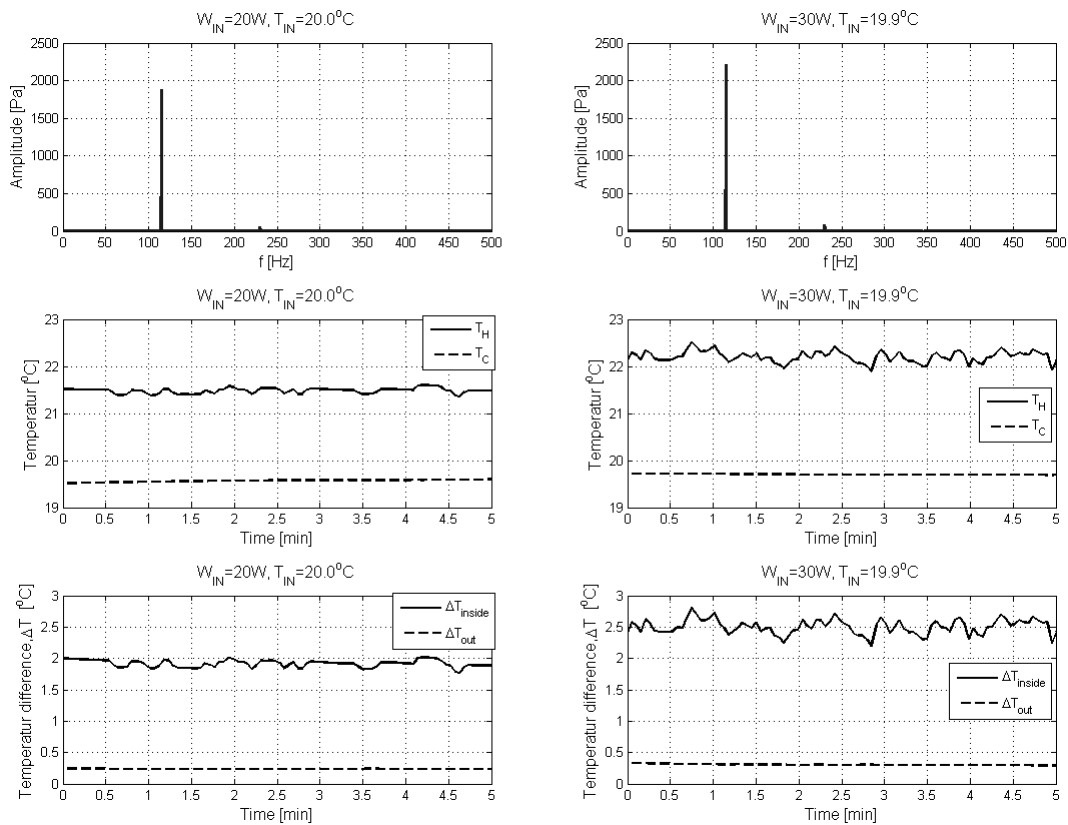


Figure A.4: Results from measurements with air, static pressure 400kPa and input power 20-30W.

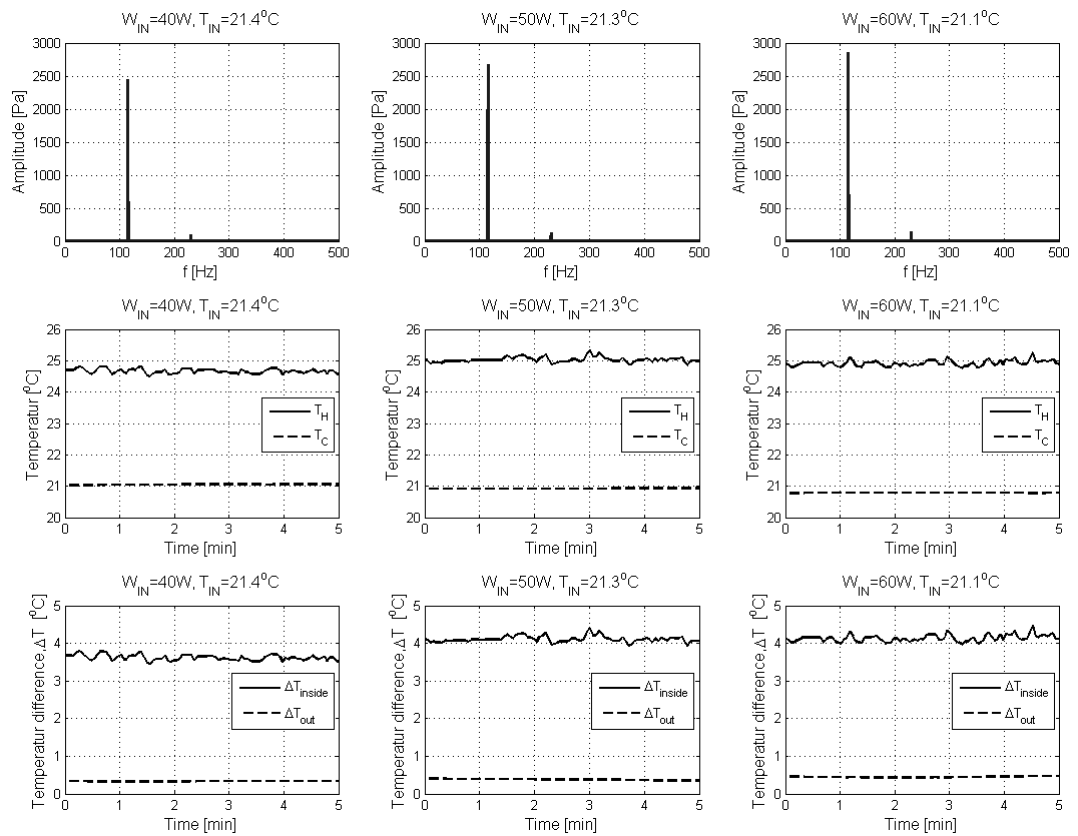


Figure A.5: Results from measurements with air, static pressure 400kPa and input power 40-60W.

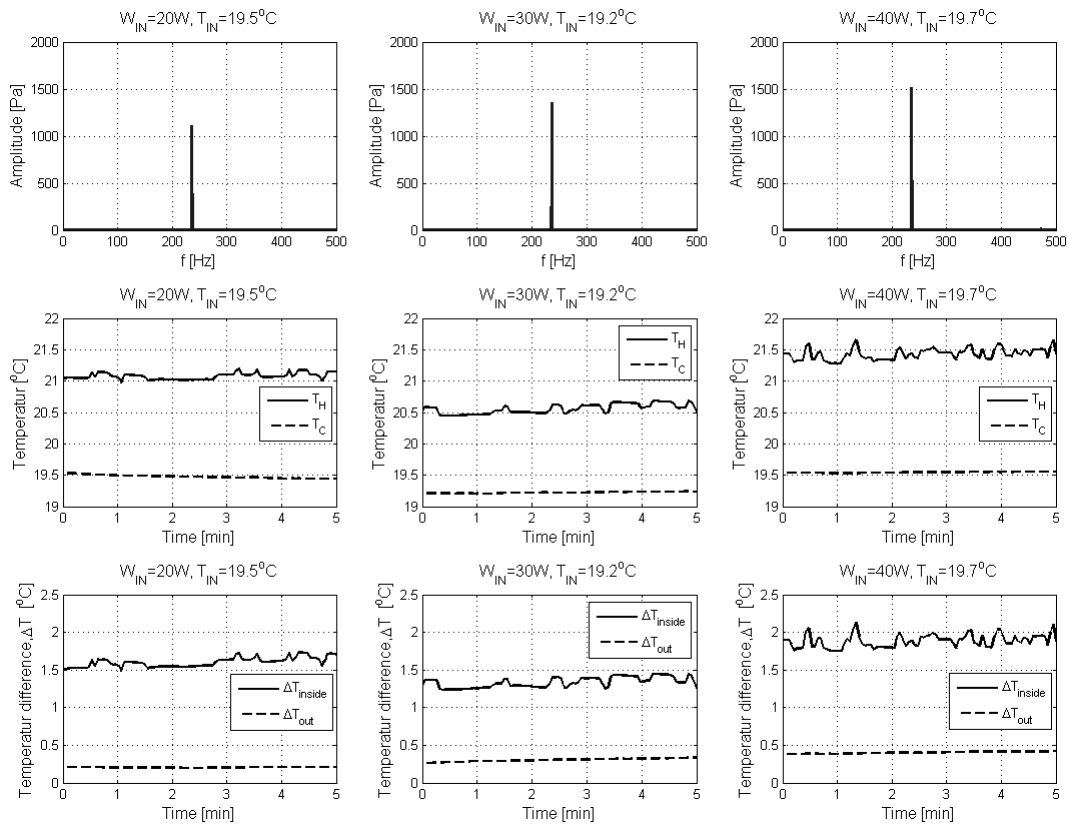


Figure A.6: Results from measurements with helium, static pressure 400kPa and input power 20-40W.